Check for updates

Within-group synchronization in the prefrontal cortex associates with intergroup conflict

Jiaxin Yang[1], Hejing Zhang[1], Jun Ni[1], Carsten K. W. De Dreu [2,3] and Yina Ma [1✉]

Individuals immersed in groups sometimes lose their individuality, take risks they would normally avoid and approach outsiders with unprovoked hostility. In this study, we identified within-group neural synchronization in the right dorsolateral prefrontal cortex (rDLPFC) and the right temporoparietal junction (rTPJ) as a candidate mechanism underlying intergroup hostility. We organized 546 individuals into 91 three-versus-three-person intergroup competitions, induced in-group bonding or no-bonding control manipulation and measured neural activity and within-group synchronization using functional near-infrared spectroscopy. After in-group bonding (versus control), individuals gave more money to in-group members than to out-group members and contributed more money to outcompete their rivals. In-group bonding decreased rDLPFC activity and increased functional connectivity between the rDLPFC and the rTPJ. Especially during the out-group attack, in-group bonding also increased within-group synchronization in both the rDLPFC and the rTPJ, and within-group rDLPFC synchronization positively correlated with intergroup hostility. Within-group synchronized reduction in prefrontal activity might explain how in-group bonding leads to impulsive and collective hostility toward outsiders.

Herding—the bottom-up alignment of thoughts or behaviors of individuals in a group—offers considerable advantages for the participating individuals[1,2]. Herding provides a level of safety that no individual can achieve alone and enables group members to achieve goals they cannot attain individually. Ant colonies and schools of fish can follow chemical signals too weak for a single individual to detect; flocking enables birds to navigate more efficiently; and human groups can outperform the best member on complex decision-making problems[1,3–5]. However, at least in humans, herding also has a dark side. Early social scientists such as LeBon (1895) and Mead (1934) typified social groups as 'madding crowds' in which anonymity and reduced feelings of individual responsibility result in deviant behavior: 'As soon as a few individuals are gathered together…the faculty of observation and the critical spirit possessed by each of them individually at once disappear'[6]. Indeed, whether we consider political protests or rioting hooligans, otherwise reasonable individuals take risks they would normally avoid and aggress outside rivals with unanticipated intensity[7–9].

Despite early suspicion that a 'mechanism of [the individual's] central nervous system'[10] and 'a connectivity of individual minds and transference of thoughts must underlie such [herding] behavior [as if] they think collectively'[11,12], little is known about the neural mechanisms underlying group-level aggression toward outsiders. In this study, we took advantage of technological innovations in brain imaging[13,14] and used functional near-infrared spectroscopy (fNIRS) to track individual brain activity and, in particular, neural synchronization among group members in relation to behavioral hostility during intergroup conflict.

Neural synchronization emerges when group members' actions or intentions are shared across brains[14] and has been proposed to mediate social contagion in which individuals mimic and align vocalizations, postures and movements with others in their group[2,14–16]. Neural synchronization within a group can emerge in distinct brain areas, such as when the areas involved in speaking and listening become synchronized between a speaker and a listener[17]. Neural synchronization in the same brain areas is observed when group members orient toward the same goal or stimuli—for example, when students focus on teacher instructions[13] or when members of a team follow leader-initiated communication[18].

If within-group neural synchronization (GNS) underlies intergroup hostility, it should be stronger in conditions known to strengthen group members' willingness to contribute to group welfare and to attack (members of) rivaling out-groups. Previous work has shown in-group cooperation and out-group aggression especially when group members ritually bond and emphasize similarity amongst them[19–21] or when the group faces an outside threat, human enemies included[1,8,22,23]. In this study, we examined these possibilities in 91 multi-round contests; each contest involved two three-person groups, group A and group D (546 participants in total, Supplementary Table 1). Individuals were fixed within groups, and groups were fixed within the contest. We applied fNIRS to simultaneously record brain activity within each group during the intergroup contest (Fig. 1a,b and Methods). The intergroup contest modeled an interaction between an attacker group A who can aggress its defender group D (Fig. 1c and Supplementary Table 2). Specifically, members of group A (D) could each contribute x (y) out of a personal financial endowment e to their group's fighting capacity C. Contributions were non-recoverable. However, when members of attacker group A collectively contributed more (i.e. $C_A = [x_1 + x_2 + x_3]$) than the members of defender group D (i.e. $C_A > C_D$, with $C_D = [y_1 + y_2 + y_3]$), group A earned all of the non-invested resources from group D (i.e. $3e – [y_1 + y_2 + y_3]$). When $C_A \leq C_D$, group D survived group A's attack, the members of both groups would keep what remained from their endowment (i.e. $e – \{x, y\}$). Thus, contributing x to C_A was personally costly but could increase personal and group gains at a cost to group D (namely, out-group attack); contributing y to C_D was personally costly as well yet served to prevent defeat and concomitant personal and group loss to group A (namely, defense)[8,23].

[1]State Key Laboratory of Cognitive Neuroscience and Learning, IDG/McGovern Institute for Brain Research, Beijing Key Laboratory of Brain Imaging and Connectomics, Beijing Normal University, Beijing, China. [2]Institute of Psychology, Leiden University, Leiden, The Netherlands. [3]Center for Research in Experimental Economics and Political Decision Making, University of Amsterdam, Amsterdam, The Netherlands. ✉e-mail: yma@bnu.edu.cn
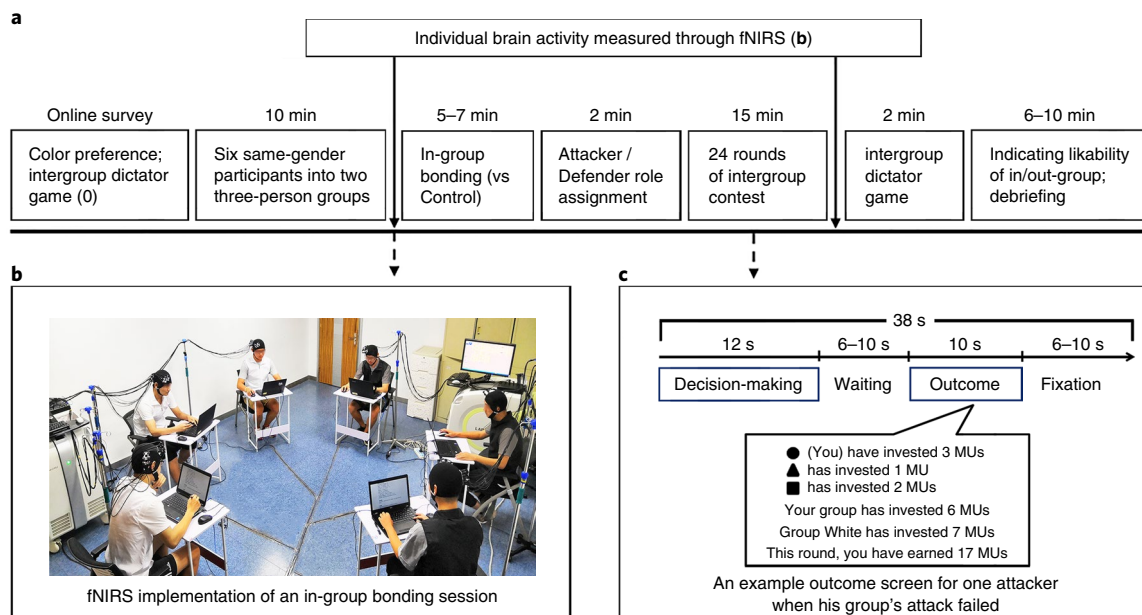
Fig. 1 | Experimental procedures. a, Timeline for an experimental session. Before coming to the laboratory, participants completed an online survey that included questionnaires, preference for the color white versus black and an online incentivized iDG (split 20 MUs between hypothetical in-group and out-group members). One to 4 d later, participants came to the laboratory in groups of six same-gender strangers, underwent the in-group bonding (or no-bonding control) exercise, were assigned to the three-person attacker or three-person defender group and made incentivized contributions to group fighting in 24 contest rounds. The experiment concluded with participants making dictator decisions between in-group and out-group members and rating the likability of in-group and out-group members. **b,** During the intergroup contest, individual neural activity in the rDLPFC and rTPJ was recorded using fNIRS. Shown here is a snapshot of an intergroup session under in-group bonding between the three-person attacker group (right, black vests, data simultaneously recorded by the same fNIRS system) and the three-person defender group (left, white vests, fNIRS data simultaneously recorded by another identical fNIRS system). **c,** Timeline of an intergroup contest round with a feedback screen for an individual in the attacker group. Individuals were fixed in their group, as were the groups, during the entire 24-round contest. Contributions were wasted, and full feedback on contributions and earnings concluded each contest round. Endowments were reset after each contest round. The duration of decision-making and outcome phases was based on a pilot experiment ($n = 24$, 11 males, age: mean $\pm$ s.d. $= 20.17 \pm 2.60$ years) where participants made self-paced decisions.

In 47 intergroup contest sessions, the three members of each A group (or D group) engaged in an in-group bonding exercise. The remaining 44 intergroup contest sessions underwent a no-bonding control manipulation. In the in-group bonding condition, the members of the same three-person group put on the same vest (black or white, i.e. the preferred color participants indicated in the pre-experiment online survey), and the members of the other group put on the opposite-colored vest (Fig. 1b). Thereafter, they engaged in a 4-min within-group chat to discover and talk about shared personal preferences. In the no-bonding control sessions, no colored vests were given, and the 4-min chat was limited to exchanging study majors and subject matters studied[21,24]. Relative to the no-bonding control, we expected in-group bonding to increase (i) intergroup discrimination, (ii) contributions to group fighting capacity and (iii) within-group neural synchronization. Furthermore, we expected (iv) GNS to associate with financial contributions to their own group's fighting capacity in the intergroup contest averaged over all 24 rounds. Because willingness to contribute to group fighting emerges endogenously when groups are under threat[1,8,22,23], we anticipated that the in-group bonding exercise would have a smaller added effect during in-group defense (i.e., in D groups) than during out-group attack (i.e., in A groups). Accordingly, we expected (v) in-group bonding effects on behavioral hostility and neural synchronization to be especially prominent during out-group attack.

Results

Behavioral displays of intergroup hostility. As predicted, participants contributed, across the 24 intergroup contest rounds, more to group fighting after in-group bonding than after the no-bonding control and during group defense rather than attack (Fig. 2a; Supplementary Table 3 gives the full statistical report of behavior indices). Earlier studies using the attacker–defender intergroup contest game also examined within-group coordination of behavior, by calculating the averaged correlation coefficients (Fisher z transformed) of 24-round contributions[23] of each pair of two participants within each group (Methods). In our study, we found that within-group behavioral coordination was better after in-group bonding and during group defense rather than attack (Fig. 2b and Supplementary Table 3). For group contributions and within-group coordination, we next explored whether winning or losing a contest round (and/or in interaction with in-group bonding) influenced next-round contributions and within-group coordination. We found that losing (versus winning) reduced next-round contributions to attack ($F_{1,87} = 22.336$, $P = 8.74 \times 10^{-6}$, $\eta^2 = 0.204$) and increased contributions to defense ($F_{1,87} = 77.894$, $P = 1.02 \times 10^{-13}$, $\eta^2 = 0.472$, Extended Data Fig. 1a). However, winning or losing a contest round did not influence next-round within-group behavioral coordination (Extended Data Fig. 1b). In neither analysis did contest outcome interact with in-group bonding.

In a final behavioral analysis, we examined indices of intergroup discrimination (Fig. 1a and Methods). After the 24-round intergroup contest, participants donated more to in-group members (in an intergroup dictator game (iDG); Fig. 2c and Methods) and expressed liking in-group members more than out-group members (Fig. 2d), especially after in-group bonding. Individuals also donated more to in-group members (Fig. 2c) and liked them better (Fig. 2d) after in-group defense rather than out-group attack (Supplementary Table 3).
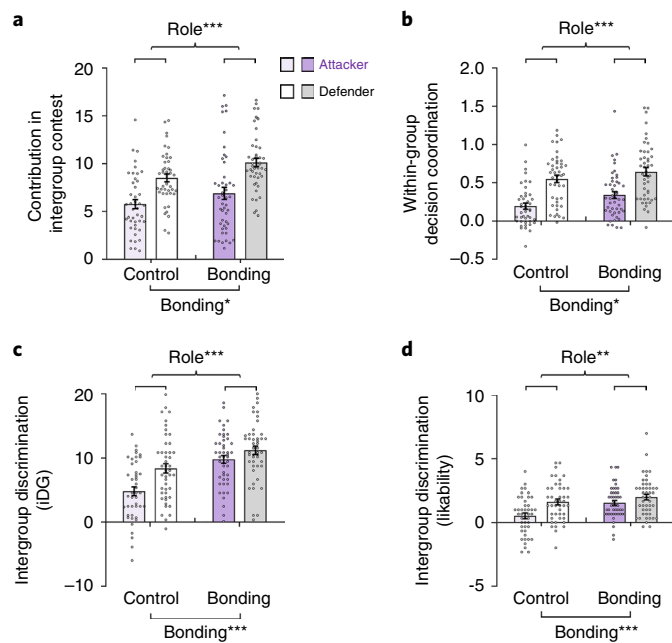
Fig. 2 | Intergroup hostility as a function of in-group bonding and group role (attack versus defense). a, **b**, Contributions to group fighting (**a**; scale, 0–20 MUs) and coordination of contributions (**b**) are higher after in-group bonding than no-bonding control (main effect of bonding, **a**, contributions: $F_{1,89} = 4.133$, $P = 0.045$, $\eta^2 = 0.044$; **b**, coordination: $F_{1,89} = 4.517$, $P = 0.036$, $\eta^2 = 0.048$) and during in-group defense rather than out-group attack (main effect of role, **a**, contributions: $F_{1,89} = 279.194$, $P = 3.48 \times 10^{-29}$, $\eta^2 = 0.758$; **b**, coordination: $F_{1,89} = 81.249$, $P = 3.52 \times 10^{-14}$, $\eta^2 = 0.477$). **c**, **d**, Intergroup discrimination in an iDG (**c**, amount of MUs donated to in-group minus that to out-group, scale, −20 to 20 MUs) and in likability ratings (**d**, likability rating of in-group members minus that of out-group members: scale, −10 to 10) is stronger after in-group bonding than no-bonding control (main effect of bonding, **c**, dictator giving: $F_{1,89} = 32.786$, $P = 1.37 \times 10^{-7}$, $\eta^2 = 0.269$; **d**, likability: $F_{1,89} = 12.625$, $P = 6.11 \times 10^{-4}$, $\eta^2 = 0.124$) and after in-group defense rather than after out-group attack (main effect of role, **c**, dictator giving: $F_{1,89} = 13.469$, $P = 4.13 \times 10^{-4}$, $\eta^2 = 0.131$; **d**, likability: $F_{1,89} = 11.386$, $P = 1.10 \times 10^{-3}$, $\eta^2 = 0.113$). Mixed-model ANOVA, $n = 91$ three-versus-three-person intergroup contest sessions (44 three-attacker and three-defender groups under no-bonding control and 47 three-attacker and three-defender groups under in-group bonding). Data are shown as the mean ± s.e. with overlaid dot plots. $^*P < 0.05$, $^{**}P < 0.01$, $^{***}P < 0.001$.

GNS. We applied fNIRS to each individual within an attacker group and its opposing defender group and thereby continuously and simultaneously measured neural activity, proxied by hemodynamic signals, within and across group members. We selected two brain regions of interest on the basis of earlier work related to (social) decision-making, cooperation and intergroup discrimination: the rDLPFC and the rTPJ (Supplementary Fig. 1 and Supplementary Table 4). The rDLPFC belongs to a group of brain regions involved in impulse inhibition and strategic decision-making[25,26]. For example, individuals with reduced prefrontal activity engage more in risky decision-making behaviors, act more impulsively and display more out-group hostility[27–29]. The rTPJ is activated when individuals consider others' thoughts and desires[30], achieve consensus decisions within a group[31], align emotions with in-group members[32] and track decisions to trust other group members, to reciprocate their cooperation and to comply with in-group norms[33,34].

GNS in our two regions of interest was operationalized in terms of wavelet transform coherence. The wavelet transform coherence

indicates the cross-correlation between two time series of concentration changes in oxygenated hemoglobin (oxy-Hb) in pairs of participants as a function of frequency and time. We averaged the coherence values from the three pairs within each three-person group to index GNS (Fig. 3a and Methods). When examining GNS, we used 14 channels (seven channels for the rDLPFC and seven channels for the rTPJ), and false discovery was mitigated using a 14-channel false discovery rate (FDR) correction for multiple comparisons (Methods).

The results showed stronger GNS in both the rDLPFC and rTPJ during decision-making compared to the period during which group members waited for outcome feedback (see Extended Data Fig. 2 for a validation analysis with comparison with pseudo groups). We expected, furthermore, stronger GNS after in-group bonding and that such an effect of in-group bonding would be stronger during group attack rather than during group defense. Indeed, GNS during the decision-making phase was modulated by bonding×role interactions in both the rDLPFC and rTPJ (Fig. 3b for an F map; rDLPFC, channel 8: $F_{1,84} = 10.765$, $P = 0.002$, $\eta^2 = 0.114$, Fig. 3c; channel 11: $F_{1,84} = 8.877$, $P = 0.004$, $\eta^2 = 0.096$, Fig. 3d; rTPJ, channel 4: $F_{1,84} = 6.810$, $P = 0.011$, $\eta^2 = 0.075$, Fig. 3e; channel 13: $F_{1,84} = 11.597$, $P = 1.02 \times 10^{-3}$, $\eta^2 = 0.121$, Fig. 3f; these channels survived a 14-channel-wise FDR correction, Supplementary Table 5a). In the no-bonding control condition, GNS was stronger during group defense than out-group attack (Fig. 3c–f and Supplementary Table 5b,c), and GNS in defender and attacker groups was similar under in-group-bonding (Supplementary Table 5b,c). Moreover, in-group bonding increased GNS during out-group attack (Fig. 3c–f and Supplementary Table 5d).

GNS might be partially due to the fact that participants were exposed to the same environment and were asked to perform the same task. To examine the possible effect of environmental and task similarity, we conducted several validation analyses. First, we generated 172 within-condition three-person pseudo groups for comparison purposes (i.e. four conditions of attacker group under in-group bonding, attacker group under no-bonding control, defender group under in-group bonding and defender group under no-bonding control; 43 three-person pseudo groups within each condition), by randomly grouping three individuals from different original, real groups under the same condition as a pseudo group (Extended Data Fig. 2c). We calculated GNS of each pseudo group in the same way as we did for the real group. To test whether the bonding×role interactions on GNS were specific to real interacting groups, we conducted role (attacker versus defender)×bonding (in-group bonding versus no-bonding control)×Group (real versus pseudo groups) ANOVA on GNS during decision-making in the four channels that showed significant bonding×role interaction in real groups. We found significant bonding×role×group interactions on GNS in rDLPFC and TPJ (all four channels survived FDR correction for the testing channels, Extended Data Fig. 3a), suggesting stronger bonding×role interaction on GNS in real interacting groups than randomly grouped individuals in the same condition. Second, we conducted nonparametric permutation tests[35,36] on the observed bonding-by-role interaction effects on GNS of the real group against the 1,000 permutation samples (each permutation sample contained 172 within-condition three-person pseudo groups). This analysis confirmed that observed bonding-by-role interaction on GNS in real groups was outside the 95% confidence interval (CI) of the permutation distribution of the 1,000 pseudo-group samples (Methods and Extended Data Fig. 3b).

Finally, we examined whether GNS in real groups might reflect just that group members made similar decisions. If so, we would expect stronger GNS when group members made more similar decisions. To examine this possibility, we computed, for each three-person group and for each contest round, the within-group decision similarity as the absolute contribution difference of each

a

b

c d e f
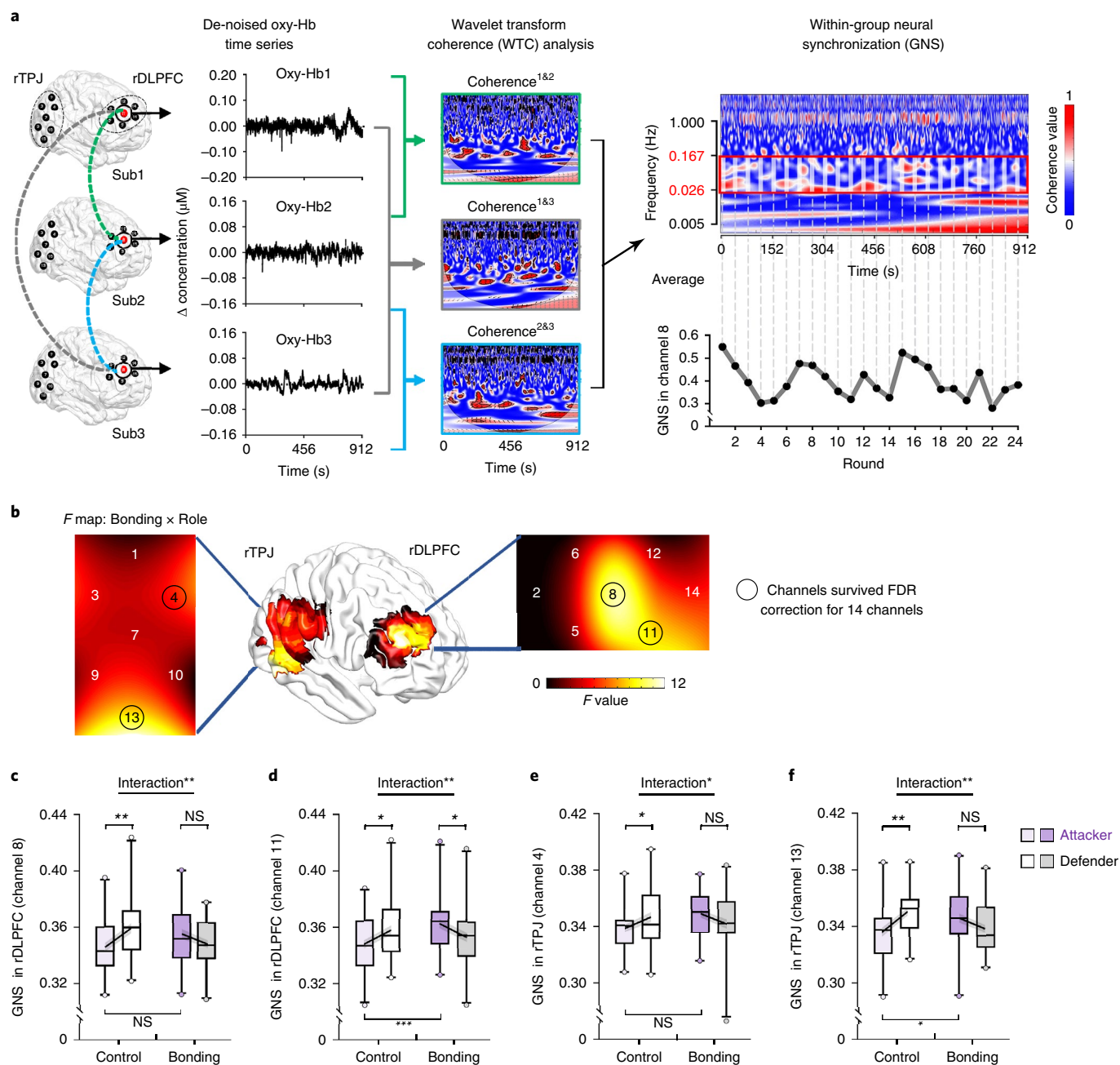
Fig. 3 | GNS as a function of in-group bonding and group role (attack versus defense). a, Illustration of the wavelet transform coherence computation to assess GNS. **b–f**, The bonding-by-role interactions on GNS in both the rDLPFC and rTPJ (channels 8 and 11 in the rDLPFC and channels 4 and 13 in the rTPJ survived FDR correction for 14 channels). Mixed-model ANOVA, $n = 86$ three-versus-three-person intergroup contest sessions. In the no-bonding control condition, GNS in the rDLPFC and rTPJ was stronger during in-group defense than during out-group attack (**c**, channel 8: $t_{42} = 3.106$, $P = 0.003$, Cohen's $d = 0.474$, 95% CI = 0.005, 0.021; **d**, channel 11: $t_{42} = 2.060$, $P = 0.046$, Cohen's $d = 0.314$, 95% CI = 1.99×10^{-4}, 0.019; **e**, channel 4: $t_{42} = 2.622$, $P = 0.012$, Cohen's $d = 0.400$, 95% CI = 0.002, 0.018; **f**, channel 13: $t_{42} = 3.141$, $P = 0.003$, Cohen's $d = 0.479$, 95% CI = 0.005, 0.023). After in-group bonding, GNS in both regions was similar during out-group attack and group defense. Two-tailed paired-samples t-tests, 43 three-person attacker groups and 43 three-person defender groups. In-group bonding increased GNS in the rDLPFC and rTPJ during out-group attack. (**c**, channel 8: $t_{84} = 1.983$, $P = 0.051$, Cohen's $d = 0.428$, 95% CI = -2.32×10^{-4}, 0.018; **d**, channel 11: $t_{84} = 3.448$, $P = 8.86 \times 10^{-4}$, Cohen's $d = 0.744$, 95% CI = 0.006, 0.022; **e**, channel 4: $t_{84} = 1.866$, $P = 0.066$, Cohen's $d = 0.402$, 95% CI = -0.001, 0.016; **f**, channel 13: $t_{84} = 2.212$, $P = 0.030$, Cohen's $d = 0.477$, 95% CI = 0.001, 0.018). Two-tailed independent-samples t-tests, 43 three-person attacker groups under in-group bonding and 43 three-person attacker groups under no-bonding control. Data are plotted as box plots for each condition, with horizontal lines indicating median values, boxes indicating 25% and 75% quartiles and whiskers indicating the 2.5–97.5% percentile range. Data points outside the range are shown separately as circles. Solid lines start from the mean and reflect the intervals of mean ± s.e. *$P < 0.05$, **$P < 0.01$, NS, not significant.

pair of the three-person group (i.e. for each round: $[(|x_1 - x_2| + |x_2 - x_3| + |x_1 - x_3|]$ for attacker groups and $[|y_1 - y_2| + |y_2 - y_3| + |y_1 - y_3|]$ for defender groups). The bonding×role interactions

remained significant when including within-group decision similarity in the analysis in the rDLPFC and the rTPJ (channel 8: $F_{1,82} = 11.166$, $P = 1.26 \times 10^{-3}$, $\eta^2 = 0.120$; channel 11: $F_{1,82} = 8.776$,

$P=0.004$, $\eta^2=0.097$; channel 4: $F_{1,82}=8.065$, $P=0.006$, $\eta^2=0.090$; channel 13: $F_{1,82}=11.024$, $P=1.34\times10^{-3}$, $\eta^2=0.119$; survived FDR correction for 14 channels, Supplementary Table 6). We categorized all the rounds into 'similar' and 'dissimilar' decisions using a median split and computed GNS as a function of bonding (in-group bonding versus no-bonding control) × role (attacker versus defender) × Similarity (similar versus dissimilar decisions). The main effect of Similarity or its interaction with role and/or bonding did not reach significance (Extended Data Fig. 4).

The two sets of validation results alone and in combination render it unlikely that the bonding × role effects on GNS in the rDLPFC and rTPJ observed in interacting groups were (exclusively) due to the fact that group members made similar decisions and/or were exposed to the same experimental environment and tasks. Accordingly, we proceeded with examining the functionality of GNS during group attack and defense. We correlated GNS with group contributions averaged across the 24 contest rounds for the four channels in which we observed the FDR-corrected bonding × role interactions (Methods). We found that stronger GNS in the rDLPFC was associated with an increase in group contributions to out-group attack (channel 8 survived FDR correction for multiple comparisons of the four channels of interest, Fig. 4a and Supplementary Table 7). GNS in the rDLPFC was associated with decreased contributions to in-group defense (Fig. 4b). A direct comparison of the association strength between attacker and defender groups (Methods) confirmed that role conditioned the relationship between GNS in the rDLPFC and contributions to group fighting ($z=4.02$, $P=5.82\times10^{-5}$, 86 three-person attacker groups and 86 three-person defender groups).

Within-group averaged neural activity. The effect of bonding and role on GNS and the association between GNS and group contribution did not indicate whether the within-group synchronized neural activity in the rDLPFC increases or decreases after in-group bonding (versus no-bonding control) and/or during in-group defense (versus out-group attack). To aid the interpretation of the role of GNS during intergroup conflict (especially at channel 8 in the rDLPFC), we examined concentration changes in oxy-Hb in individual brain activity in the rDLPFC (averaged across three participants within the same group, Extended Data Fig. 5a). We found that rDLPFC activity was lower in the in-group bonding condition than in the no-bonding control condition (Fig. 5a). Next, we regressed the group contribution on round T (GC_T) on rDLPFC activity on the last round ($T-1$). This analysis showed that reduced rDLPFC activity predicted increased contributions on the next round ($\beta=-0.051$, $t_{85}=-2.958$, $P=0.004$, Cohen's $d=-0.319$, 95% $CI=-0.085$, -0.017; $n=86$ three-versus-three-person intergroup contest sessions).

We concluded our analyses by exploring the functional connectivity between our two regions of interest. To index group-averaged functional connectivity (GFC) between the rDLPFC and the rTPJ, we performed coherence analyses[37] between the rDLPFC and the rTPJ for each individual and averaged the coherence values across the three participants within the same group (Extended Data Fig. 5b). In-group bonding (versus no-bonding control) increased the functional connectivity between the rDLPFC and the rTPJ (Fig. 5b for the grand mean rDLPFC–rTPJ connectivity; Fig. 5c for channel-pairwise rDLPFC–rTPJ connectivity) (18 rDLPFC–rTPJ channel pairs survived FDR correction for 49 rDLPFC–rTPJ channel pairs, Extended Data Fig. 6 and Supplementary Table 8).

Discussion

Previous studies showed that in-group bonding increases an individual's commitment to and identification with the group[38], enabling personally costly behavior that serves the in-group[39] and that discriminates and punishes (members of) rivaling out-groups[7,40].
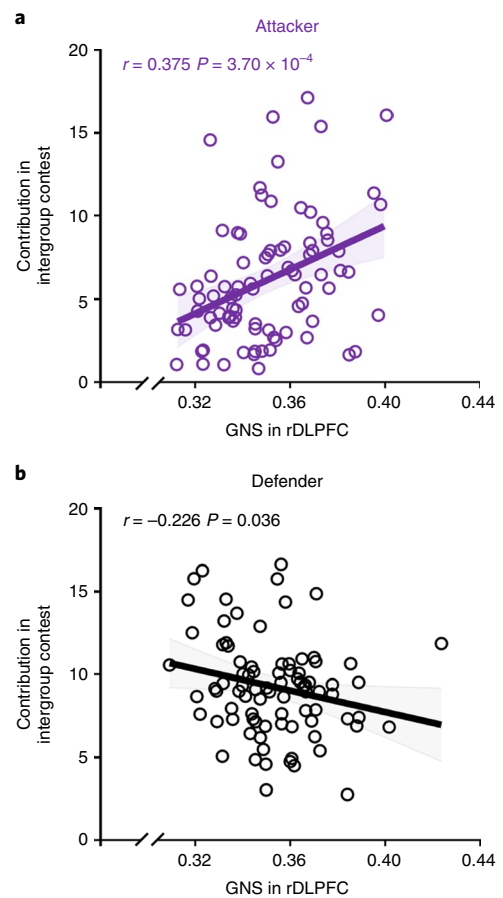
Fig. 4 | GNS in the rDLPFC (channel 8) correlates with intergroup hostility. GNS in the rDLPFC associates with (**a**) increased contributions to out-group attack (channel 8 survived FDR correction for multiple comparisons of the four channels of interest, Pearson's $r=0.375$, $P=3.7\times10^{-4}$, 95% $CI=0.174, 0.576$, $n=86$ three-person attacker groups) and (**b**) decreased in-group defense (Pearson's $r=-0.226$, $P=0.036$, 95% $CI=-0.438, -0.015$, $n=86$ three-person defender groups). Correlations were performed by Pearson's correlation coefficient analysis. Each circle depicts a single three-person group's contribution to the intergroup contest (y coordinate) and GNS in the rDLPFC (x coordinate). Each solid line represents the least squares fit, with shading showing the 95% CI.

To this psychological theory, our study adds information about the neural mechanisms involved, both at the level of individual group members and at the level of the group. Specifically, we found that in-group bonding enhanced within-group coordination, increased personally costly contributions to the in-group's ability to compete against the out-group (henceforth fighting capacity), reduced neural activity in the DLPFC and increased functional connectivity between the DLPFC and the TPJ. Furthermore, and fitting early speculation by social scientists concerning de-individuated group minds and herd hostility[2,6], we found that in-group bonding influenced GNS in both the DLPFC and the TPJ, and that synchronization in the DLPFC was associated with intergroup hostility.

The effect of in-group bonding on GNS in the rDLPFC differed between attacker and defender groups. In-group bonding in attacker groups increased GNS, and greater GNS was correlated with increased contributions to out-group attack. By contrast, in defender groups, in-group bonding reduced GNS, and GNS was negatively correlated with contributions to defense. To interpret these results, we assumed that (1) reduced activity in the rDLPFC is associated with less controlled and more impulsive and riskier
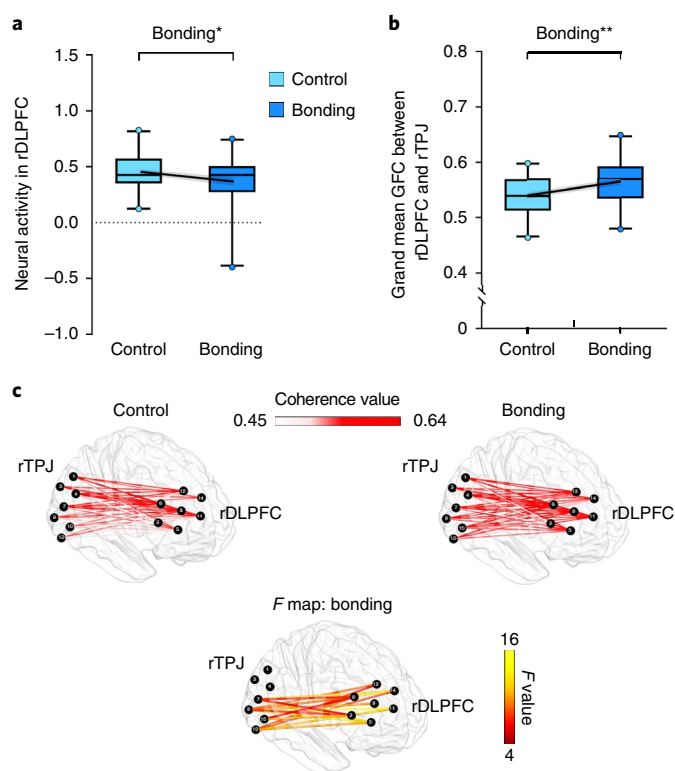
Fig. 5 | Influence of in-group bonding on within-group averaged rDLPFC activity and group-averaged functional connectivity of rDLPFC–rTPJ. a, In-group bonding (versus no-bonding control) reduced neural activity in the rDLPFC ($F_{1,84} = 4.151$, $P = 0.045$, $\eta^2 = 0.047$; shown are within-group averaged oxy-Hb concentration changes [decision-making phase − waiting phase]). **b**, **c**, In-group bonding (versus no-bonding control) increased functional connectivity of rDLPFC–rTPJ. **b**, Grand mean rDLPFC–rTPJ connectivity ($F_{1,84} = 9.035$, $P = 0.003$, $\eta^2 = 0.097$). **c**, Channel-pairwise rDLPFC–rTPJ connectivity (18 rDLPFC–rTPJ channel pairs survived FDR correction for 49 rDLPFC–rTPJ channel pairs). The grand mean rDLPFC–rTPJ connectivity was indexed by the averaged coherence value of 49 channel pairs between the right rDLPFC (i.e., seven channels within the rDLPFC) and rTPJ (i.e., seven channels within the rTPJ) within three-person groups. Mixed-model ANOVA, $n = 86$ three-versus-three-person intergroup contest sessions (43 sessions under no-bonding control and 43 sessions under in-group bonding). Data are plotted as box plots for each condition, in which horizontal lines indicate median values, boxes indicate 25% and 75% quartiles and whiskers indicate the 2.5–97.5% percentile range. Data points outside the range are shown separately as circles. Solid lines start from the mean and reflect the intervals of mean ± s.e. *$P < 0.05$, **$P < 0.01$.

decision-making behaviors[27–29]; (2) risk-taking translates to higher contributions to out-group attack (i.e. gambling on victory with the risk of losing resources) and lower contributions to defense[41,42] (i.e. gambling on saving resources with the risk of losing them all); and (3) attacker groups initiate intergroup conflict—they 'set the tone'—whereas defender groups are adapting to the (threat of) out-group attacks[42,43]. If these assumptions are valid, our results suggest that in-group bonding not only increases group commitment but also increases the willingness to take personal risks. Our results suggest that, during out-group attack, these two mechanisms operate in parallel, so that both group commitment and risk tolerance increase an individual's contribution to group fighting capacity. In-group bonding increased GNS and reduced activity in the rDLPFC during out-group attack. However, during in-group defense, group commitment and impulsivity increased contributions to fight against out-group attacks, but risk tolerance might

reduce these contributions. In addition, the defender group members' decisions on how much to contribute to the group pool were mainly in response to (expected) out-group attacks, which might explain why in-group bonding had weak and inconsistent effects on behavior and neural measures during group defense.

Two sets of additional findings further inform about the role of activity in the rDLPFC and rTPJ during intergroup interaction. First, we found that winning or losing a contest round had no effect on within-group behavioral coordination (Extended Data Fig. 1b) or GNS (Extended Data Fig. 7). Losing a contest round did, however, increase rDLPFC activity for both attacker and defender groups in next-round decision-making (Extended Data Fig. 8) and was linked with reduced contributions to out-group attack and increased contributions to in-group defense (Extended Data Fig. 1a). Together, these findings suggest that, in both attackers and defenders, losing a contest round increases impulse inhibition and risk aversion, which is mediated by increased activity in the rDLPFC[27–29]. Second, we found that in-group bonding increased functional connectivity between the rDLPFC and rTPJ. The DLPFC has been associated with strategic deliberation and controlled decision-making[44,45], and the TPJ has been implicated in mentalizing and collective decision-making[30,31]. As such, the increased rDLPFC–rTPJ connectivity after in-group bonding observed in our study fits with the idea that group herding might reflect 'social alignment' between the observation and execution systems in the human brain[16]. Such social alignment allows for the functional integration of social information into collective decisions[31,46,47]. Perhaps in-group bonding facilitates group members' willingness to understand and integrate other group members' intentions into their own behavioral strategy[30,44], which, in turn, might facilitate coordinated collective action[30,31].

The idea that within-group synchronization in the rDLPFC and rTPJ tracks a de-individuated, impulsive 'group mind' presumes that brain-to-brain coupling is not explained by the fact that participants were in the same (experimental) environment and were performing the same (experimental) tasks. We provided evidence that this is indeed not the case. First, we note that interaction-specific neural synchronization during real-time social interaction is distinct from similar neural responses that occur when performing the same task at the same time[48,49]. Specifically, similar neural activity refers only to similar amplitude of activity, whereas neural synchronization refers to a phase-locked correlation derived from wavelet coherence analysis. Indeed, as shown, decision (dis)similarity did not modulate the results of GNS. Second, we ensured that the experimental environment and tasks were highly similar across the four experimental conditions. Third, comparison with pseudo groups showed that effects of in-group bonding and attacker/defender role on GNS occured only in our real interacting groups and not in pseudo groups that were exposed to the same environment, tasks and experimental treatments yet did not interact during decision-making and feedback. Taken together, we can conclude that GNS in the rDLPFC and rTPJ provides a neural marker of the 'group mind'.

To the extent that contributing to intergroup contests mimics what social scientists identified as herd hostility[6,10], GNS of reduced rDLPFC activity might be a mechanism that enables 'a connectivity of individual minds and transference of thoughts'[11,12] and underlying herding behavior and impulsive and risky group-level hostility. At the same time, extrapolating from experimental results to real-world intergroup violence is nontrivial. Accordingly, rather than offering conclusive evidence about the mechanisms responsible for herd hostility, our findings point to the possibility that GNS contributes to this arguably dark side of immersing in human groups—impulsive and risky out-group hostility and discrimination[7–9]. The same applies to our findings for in-group bonding and increased contributions to group attacks on outside rivals. It is noteworthy, however, that groups preparing for tribal raids and warfare engage in ritual bonding and build close friendships[19,20]. Our findings suggest that

such age-old practices align individual group members not only in their behavioral orientation but also in the shared downregulation of neural activity involved in self-preservation and risk aversion. If true, herd hostility reflects disinhibited tolerance for risk that might be personally costly but beneficial to one's group.

Online content

Any methods, additional references, Nature Research reporting summaries, source data, extended data, supplementary information, acknowledgements, peer review information; details of author contributions and competing interests; and statements of data and code availability are available at https://doi.org/10.1038/s41593-020-0630-x.

References

1. Hamilton, W. D. Geometry for the selfish herd. *J. Theor. Biol.* **31**, 295–311 (1971).
2. Raafat, R. M., Chater, N. & Frith, C. Herding in humans. *Trends Cogn. Sci.* **13**, 420–428 (2009).
3. Flack, A., Nagy, M., Fiedler, W., Couzin, I. D. & Wikelski, M. From local collective behavior to global migratory patterns in white storks. *Science* **360**, 911–914 (2018).
4. Laughlin, P. R., Hatch, E. C., Silver, J. S. & Boh, L. Groups perform better than the best individuals on letters-to-numbers problems: effects of group size. *J. Pers. Soc. Psych.* **90**, 644–651 (2006).
5. Woolley, A. W., Chabris, C. F., Pentland, A., Hashmi, N. & Malone, T. W. Evidence for a collective intelligence factor in the performance of human groups. *Science* **330**, 686–688 (2010).
6. Le Bon, G. *The Crowd: A Study of the Popular Mind* (Macmillan, 1968).
7. Choi, J. K. & Bowles, S. The coevolution of parochial altruism and war. *Science* **318**, 636–640 (2007).
8. De Dreu, C. K. et al. In-group defense, out-group aggression, and coordination failure in intergroup conflict. *Proc. Natl Acad. Sci. USA* **113**, 10524–10529 (2016).
9. Postmes, T. & Spears, R. Deindividuation and antinormative behavior: a meta-analysis. *Psych. Bull* **123**, 238–259 (1998).
10. Mead, G. H. *Mind, Self, and Society* (University of Chicago Press, 1934).
11. Selous, E. *Bird Life Glimpses.* (G. Allen, 1905).
12. Couzin, I. Collective minds. *Nature* **445**, 715 (2009).
13. Dikker, S. et al. Brain-to-brain synchrony tracks real-world dynamic group interactions in the classroom. *Curr. Biol.* **7**, 1375–1380 (2017).
14. Hasson, U. & Frith, C. D. Mirroring and beyond: coupled dynamics as a generalized framework for modelling social interactions. *Phil. Trans. R. Soc. B* **371**, 1693–1702 (2016).
15. Echterhoff, G., Higgins, E. T. & Levine, J. M. Shared reality: experiencing commonality with others' inner states about the world. *Perspect. Psychol. Sci.* **4**, 496–521 (2009).
16. Shamay-Tsoory, S. G., Saporta, N., Marton-Alper, I. Z. & Gvirts, H. Z. Herding brains: a core neural mechanism for social alignment. *Trends Cogn., Sci.* **23**, 174–186 (2019).
17. Stephens, G. J., Silbert, L. J. & Hasson, U. Speaker-listener neural coupling underlies successful communication. *Proc. Natl. Acad. Sci. USA.* **107**, 14425–14430 (2010).
18. Jiang, J. et al. Leader emergence through interpersonal neural synchronization. *Proc. Natl. Acad. Sci. USA.* **112**, 4274–4279 (2015).
19. Gould, R. V. Collective violence and group solidarity: evidence from a feuding society. *Am. Soc. Rev* **22**, 356–380 (1999).
20. Glowacki, L. et al. Formation of raiding parties for intergroup violence is mediated by social network structure. *Proc. Natl Acad. Sci. USA.* **113**, 12114–12119 (2016).
21. Efferson, C., Lalive, R. & Fehr, E. The coevolution of cultural groups and in-group favoritism. *Science* **321**, 1844–1849 (2008).
22. De Dreu, C. K. et al. The neuropeptide oxytocin regulates parochial altruism in intergroup conflict among humans. *Science* **328**, 1408–1411 (2010).
23. Zhang, H., Gross, J., De Dreu, C. K. & Ma, Y. Oxytocin promotes coordinated out-group attack during intergroup conflict in humans. *Elife* **8**, e40698 (2019).
24. Ma, Y., Liu, Y., Rand, D. G., Heatherton, T. F. & Han, S. Opposing oxytocin effects on intergroup cooperative behavior in intuitive and reflective minds. *Neuropsychopharmacology* **40**, 2379–2387 (2015).
25. Gläscher, J. et al. Lesion mapping of cognitive control and value-based decision making in the prefrontal cortex. *Proc. Natl Acad. Sci. USA.* **109**, 14681–14686 (2012).
26. Wang, X. J. Decision making in recurrent neuronal circuits. *Neuron* **60**, 215–234 (2008).
27. Knoch, D. et al. Disruption of the right prefrontal cortex by low-frequency repetitive transcranial magnetic stimulation induces risk-taking behavior. *J. Neurosci.* **26**, 6469–6472 (2006).
28. Knoch, D., Pascual-Leone, A., Meyer, K., Treyer, V. & Fehr, E. Diminishing reciprocal fairness by disrupting the right prefrontal cortex. *Science* **314**, 829–832 (2006).
29. Cikara, M., Jenkins, A. C., Dufour, N. & Saxe, R. Reduced self-referential neural response during intergroup competition predicts competitor harm. *Neuroimage* **96**, 36–43 (2014).
30. Carter, R. M. & Huettel, S. A. A nexus model of the temporal-parietal junction. *Trends Cogn. Sci.* **17**, 328–336 (2013).
31. Suzuki, S., Adachi, R., Dunne, S., Bossaerts, P. & O'Doherty, J. P. Neural mechanisms underlying human consensus decision-making. *Neuron* **86**, 591–602 (2015).
32. Lin, L., Qu, Y. & Telzer, E. H. Intergroup social influence on emotion processing in the brain. *Proc. Natl Acad. Sci. USA* **115**, 10630–10635 (2018).
33. Prochazkova, E. et al. Pupil mimicry promotes trust through the theory of mind network. *Proc. Natl Acad. Sci. USA* **115**, E7265–E7274 (2018).
34. Baumgartner, T., Schiller, B., Rieskamp, J., Gianotti, L. R. & Knoch, D. Diminishing parochialism in intergroup conflict by disrupting the right temporo-parietal junction. *Soc. Cogn. Affect. Neurosci.* **9**, 653–660 (2014).
35. Holmes, A. P., Blair, C. R., Watson, J. D. & Ford, I. Nonparametric analysis of statistic images from functional mapping experiments. *J. Cereb. Blood Flow Metab.* **16**, 7–22 (1996).
36. Nichols, T. E. & Holmes, A. P. Nonparametric permutation tests for functional neuroimaging: a primer with examples. *Hum. Brain Map.* **15**, 1–25 (2002).
37. Zhang, L., Sun, J., Sun, B., Luo, Q. & Gong, H. Studying hemispheric lateralization during a Stroop task through near-infrared spectroscopy-based connectivity. *J. Biomed. Opt.* **19**, 057012 (2014).
38. Brewer, M. B., Manzi, J. M. & Shaw, J. S. In-group identification as a function of depersonalization, distinctiveness, and status. *Psychol. Sci.* **4**, 88–92 (1993).
39. Whitehouse, H. Dying for the group: towards a general theory of extreme self-sacrifice. *Behav. Brain Sci.* https://doi.org/10.1017/S0140525X18000249 (2018).
40. Bernhard, H., Fischbacher, U. & Fehr, E. Parochial altruism in humans. *Nature* **442**, 912–915 (2016).
41. Chowdhury, S. M. The attack and defense mechanisms–perspectives from behavioral economics and game theory. *Behav. Brain Sci.* **42**, e121 (2019).
42. De Dreu, C. K. & Gross, J. Revisiting the form and function of conflict: neurobiological, psychological, and cultural mechanisms for attack and defense within and between groups. *Behav. Brain Sci.* **42**, e116 (2019).
43. Wrangham, R. W. Two types of aggression in human evolution. *Proc. Natl Acad. Sci. USA* **115**, 245–253 (2018).
44. Yamagishi, T., Takagishi, H., Fermin, A. D., Kanai, R., Li, Y. & Matsumoto, Y. Cortical thickness of the dorsolateral prefrontal cortex predicts strategic choices in economic games. *Proc. Natl Acad. Sci. USA* **113**, 5582–5587 (2016).
45. Steinbeis, N., Bernhardt, B. C. & Singer, T. Impulse control and underlying functions of the left DLPFC mediate age-related and age-independent individual differences in strategic social behavior. *Neuron* **73**, 1040–1051 (2012).
46. Piva, M., Zhang, X., Noah, J. A., Chang, S. W. & Hirsch, J. Distributed neural activity patterns during human-to-human competition. *Front. Hum. Neurosci.* **11**, 571 (2017).
47. Yu, H., Li, J. & Zhou, X. Neural substrates of intention–consequence integration and its impact on reactive punishment in interpersonal transgression. *J. Neurosci.* **35**, 4917–4925 (2015).
48. Schilbach, L. et al. Toward a second-person neuroscience. *Behav. Brain Sci.* **36**, 393–414 (2013).
49. Redcay, E. & Schilbach, L. Using second-person neuroscience to elucidate the mechanisms of social interaction. *Nat. Rev. Neurosci.* **20**, 495–505 (2019).

Methods

Participants and ethics. Healthy individuals (558 participants, 252 males, age 18–30 years, mean ± s.d. = 22.06 ± 2.58 years) were invited as paid volunteers. All participants had normal or corrected-to-normal vision and no history of neurological or psychiatric disorders. Those who majored in psychology or economics or participated in any similar study were excluded from participation. The experiment involved no deception, and participants were paid a $10 show-up fee plus their average earnings in two randomly selected (out of 24) contest rounds. The experimental protocols adhered to the standards set by the Declaration of Helsinki and were approved by a local research ethics committee at the State Key Laboratory of Cognitive Neuroscience and Learning, Beijing Normal University, Beijing, China (protocol IORG0004944, OSF: https://osf.io/uh3sx/). All participants provided written informed consent to participate after the experimental procedures had been fully explained and acknowledged their right to withdraw at any time during the study.

The sample size was determined a priori using G*Power 3.1 (ref. [50]) to estimate the number of six-person sessions needed to detect significant effects with 80% statistical power. We originally considered conducting power analysis on the basis of both behavioral and neural effects. However, most fNIRS studies have considered dyad-level interactions, and only a few[18,51,52] have examined neural synchronization in single groups with group sizes with $n \geq 3$, and we are unaware of fNIRS studies examining intergroup (economic) interaction. We thus calculated a priori sample size estimates on the basis of earlier behavioral studies using the intergroup contest that we also used here. Based on a small-to-medium effect size estimated by a meta-analysis on the effect of in-group bonding on intergroup discrimination in cooperation (Cohen's $d = 0.32$)[53], 80 six-person sessions were needed to detect a reliable effect with $\alpha = 0.05$ and $\beta = 0.80$ for a within (attacker versus defender) by between (in-group bonding versus no-bonding control) treatment interaction. To allow for dropout due to technical failure, we recruited 93 sessions. Two six-person intergroup contest sessions were excluded because of a technical failure to record contribution decisions, leaving 546 participants in 91 intergroup contest sessions (40 male sessions, mean ± s.d. = 22.04 ± 1.31 years, Supplementary Table 1a) for behavioral data analysis. Another five six-person intergroup contest sessions were excluded because of technical failure with fNIRS measurements, leaving a total of 516 participants in 86 intergroup contest sessions for neural data analysis (38 male sessions, mean ± s.d. = 22.01 ± 1.29 years, Supplementary Table 1b). Despite these deletions, the final sample size exceeded those typically used in studies focusing on (dyadic or group) neural synchronization. The attacker and defender groups under in-group bonding or no-bonding control conditions did not differ in gender, age, education, empathic capacity, cooperative personality, social value orientation, prosocial personality, impulsiveness, justice sensitivity, preference for social hierarchy or baseline intergroup discrimination (Supplementary Table 1).

Experimental procedures and tasks. Before coming to the laboratory, participants completed an online survey including a set of questionnaires (Supplementary Table 1). They also indicated their preference for the color white versus black that we used for the in-group bonding manipulation. At least 1 d (range, 1–4 d) later, participants came to the laboratory for the main experiment in groups of six same-gender strangers and were randomly assigned to the three-person group A or D. Participants randomly underwent the in-group bonding or no-bonding control manipulation, made contributions in 24 rounds of the intergroup contest during hyperscanning with fNIRS and then made dictator giving decisions in an iDG[54] (where participants split 20 monetary units (MUs) between in-group members and out-group members). Upon completion of the dictator giving, participants rated the likability of others in their own group and those in the opposing group.

In-group bonding manipulation. To manipulate in-group bonding, we merged three procedures used in previous studies[21,24]. First, for each in-group bonding session, we invited three participants preferring black and another three preferring white (as indicated with the online survey) and used this color preference to create group identities, with the individuals preferring black over white being labeled as 'Group Black' and those preferring white over black being labeled as 'Group White'. Each participant was then given either a black vest (for 'Group Black') or a white vest (for 'Group White') to wear during the rest of the experimental session[21,24]. Finally, each three-person group was given 4-min online chatting with each other to introduce themselves and find three-person-shared features[55]. Group Black and Group White were randomly assigned to the role of attacker or defender in the intergroup contest game. In the no-bonding control sessions, similar to previous studies[56], we did not provide a group uniform, and during the 4-min online chatting, individuals were asked to talk about the main courses they had been taking during this semester without being explicitly asked to find shared features.

To examine and quantify the effect of the in-group bonding manipulation on increasing intergroup discrimination, participants made allocation decisions in an iDG where they split 20 MUs between in-group members and out-group members[54] and rated the likability of others in their own group and those in the opposing group[24]. We compared intergroup discrimination in the iDG before and after the bonding manipulation. Before the bonding manipulation, participants in both conditions showed a similar level of intergroup discrimination (Extended

Data Fig. 9a). After in-group bonding (relative to the no-bonding control), intergroup discrimination increased in both attacker and defender groups (Extended Data Fig. 9b,c).

Intergroup contest game. The intergroup contest game is a dynamic, fully incentivized contest game with real-time feedback between a three-person attacker group (group A) and a three-person defender group (group D)[8,23]. Each intergroup contest session involved 24 contest rounds with full reset and real-time feedback between rounds (Fig. 1 and Supplementary Table 2). Participants were first shown the instructions screen describing the intergroup contest game. We used neutral language and avoided terms such as defense and attack. Understanding of the instructions was verified with two comprehension questions. Thereafter, participants made contribution decisions in 24 rounds. For each contest round (Fig. 1c), participants were first given 12 s to decide how much to contribute to the group pool (henceforth the group decision-making phase). If participants did not respond within the time period (0.28% of the contest rounds across all sessions), the contribution would be a random number generated by the computer. Upon entering their contribution, participants saw a waiting screen for a jittered time interval of 6–10 s (8 s on average), followed by a 10-s outcome screen presenting feedback on (1) the contribution of each individual in their own group (participants were identified by shape labels); (2) one's own and the rival's group-level contribution (i.e. C_A and C_D); and (3) the contest round's payoff (Fig. 1c). The outcome screen was followed by an 8-s inter-round interval (6–10 s). The total duration of wait screen and inter-round interval was fixed to 16 s, and each round lasted for 38 s in total (the time intervals were predetermined in our earlier study[23] and in a pilot experiment (Fig. 1c)) to ensure ample time for contribution decisions and the processing of outcome feedback.

fNRIS data acquisition. We employed two identical LABNIRS optical topography systems (52-channel high-speed LABNIRS, Shimadzu) to simultaneously collect imaging data from the six participants in each intergroup contest session, with each system recording the three participants sharing the same role. The fNIRS signals were acquired at a sampling rate of 47.62 Hz and later downsampled to 9.52 Hz by averaging five consecutive data points for all the analyses to decrease temporal autocorrelation[57]. For each participant, we used two identical 3×2 optode probe sets, with each probe set consisting of three light emitters and three detectors (inter-optode distance of 30 mm) and seven channels (illustrated in Supplementary Fig. 1). The probe sets were separately placed on the rTPJ and the rDLPFC according to the relevant standard positions of P6 and F4 in the international 10/10 system for electroencephalogram electrode placement[58,59]. To further confirm the position of the optode probe sets, the high-resolution T1-weighted structural images from six participants were acquired using a 3T Siemens Trio scanner at the MRI Research Centre, Beijing Normal University ($256 \times 256 \times 144$ matrix with a spatial resolution of $1 \times 1 \times 1.33$ mm, repetition time = 2,530 ms, echo time = 3.39 ms, inversion time = 1,100 ms, flip angle = 7°). Supplementary Table 4 shows the anatomical coordinates of each optode, further confirming the anatomical localization of rTPJ and rDLPFC.

We measured the relative changes of absorbed near-infrared light at three wavelengths of 780 nm, 805 nm and 830 nm. These changes were transformed into the relative concentration changes of oxy-Hb, deoxygenated hemoglobin (deoxy-Hb) and total hemoglobin using a modified Beer–Lambert law[60], allowing measurement of brain activity[61]. The current study focused only on the concentration changes of oxy-Hb, given it to be the most sensitive indicator of the regional cerebral blood flow in fNIRS measures. Increases in oxy-Hb have been recognzed as the consequence of neural activity and corresponding to the blood oxygenation level dependent signal measured by fMRI[62–64].

Behavioral data analysis. Data were aggregated at the three-person group level and submitted to ANOVA with role (attacker versus defender) as a within-subjects factor and bonding (in-group bonding versus no-bonding control) as a between-subjects factor. We analyzed (1) contribution averaged within the three-person group and across 24 rounds (range, 0–20 MUs); (2) within-group decision coordination (GDC); (3) dictator giving to in-group and out-group members; and (4) likability ratings of in-group and out-group members (see Supplementary Table 3 for the full statistical reports). GDC was calculated by correlating the 24-round contributions of each pair of two participants within each three-person group (resulting in three correlations per group) and averaging the three Fisher z-transformed correlation coefficients. Higher GDC values thus indicate higher levels of similarity at the round-level contributions between the three members in a group, which we took as a proxy for group-level coordination in contribution decisions[8,23]. For dictator giving and likability ratings, we computed an index of intergroup discrimination by subtracting donations (likability ratings) given to out-group members from those given to in-group members.

fNIRS data analysis. We calculated three neural indices for the current study: GNS (i.e. interpersonal brain activities that co-vary along the time course, Fig. 3a), neural activity of a single brain (Extended Data Fig. 5a) and rDLPFC–rTPJ function connectivity (Extended Data Fig. 5b). To remove systemic noise, we first employed a wavelet-based method to remove global noise[65], as the

wavelet transform was used as a powerful mathematical tool in fNIRS data pre-processing[66,67]. Specifically, similar to previous studies[65], we used wavelet transform coherence to automatically identify and quantify global physiological components per channel and then extracted them out of the hemodynamic signals by a wavelet algorithm. This de-noising method deals with both the spatial distribution and time variance of physiological noise among different channels and is effective in capturing globally co-varying time-frequency components. After wavelet-based global noise removal, we calculated the GNS and within-group averaged neural activity. Alternatively, we also analyzed the data in another way that was similar to previous studies[68] where we did not apply global noise removal but included global mean covariance (i.e. the mean values across conditions and across all 14 channels) as a covariate in our model and found that the observed effects remained reliable (Supplementary Table 9).

With regard to GNS, and similar to previous studies[18,69], we employed the wavelet transform coherence analysis to calculate the cross-correlation between two oxy-Hb time series of pairs of participants as a function of frequency and time[70]. Within each three-person group sharing the same role in the intergroup contest game (taking one three-person group with subject IDs of 1, 2 and 3 as an example), we used the same fNIRS system to simultaneously acquire three same-length oxy-Hb time series for each channel (referred to as oxy-Hb$_1$, oxy-Hb$_2$ and oxy-Hb$_3$). After global noise removal, we then applied wavelet transform coherence analysis to each pair of three oxy-Hb time series and generated three time-frequency two-dimensional matrices of the coherence values for each three-person group (Coherence$_{1\&2}$, Coherence$_{1\&3}$ and Coherence$_{2\&3}$). We averaged three coherence values from three pairs as the group-level coherence value for each three-person group. In each group time-frequency matrix (Fig. 3a), each line corresponded to a specific frequency point, each column corresponded to a specific time point and the color bar corresponded to the coherence value.

Previous studies determined the frequency band for the wavelet coherence analysis based on the inverse of the time interval between two continuous trials[71,72] or task-related events[57,69,73]. In the current intergroup contest game, each trial lasted for 38 s (i.e. the total length of one round), and the shortest duration of a single event in each trial was 6 s. Thus, similar to previous studies, we identified a frequency band of interest according to the timeline for each intergroup contest round (i.e. a frequency band from 0.0263 Hz to 0.1667 Hz, corresponding to the period between 6 s and 38 s). Visual inspection of the group-averaged wavelet transform coherence graph, as illustrated in Fig. 3a, confirmed higher coherence values within this frequency band. This frequency band also excluded high- and low-frequency noise, including that related to respiration (around 0.2–0.3 Hz) and cardiac pulsation (around 1 Hz), all of which might lead to artificial coherence. For each channel, the average coherence values were computed for each intergroup contest round in the frequency band of interest (i.e. 0.0263–0.1667 Hz).

For further analysis, we defined three time segments for each contest round: a 12-s group decision-making phase, an on-average 8-s (6–10 s) waiting screen phase and a 10-s outcome screen phase. The average coherence values were computed for each of these segments in the frequency band of interest to indicate GNS for each phase of each contest round, which was then Fisher z transformed and submitted to the round-level analysis for GNS (Fig. 3a). Moreover, we averaged the GNS across all intergroup contest rounds for each channel and entered the round-aggregated GNS into 2 (bonding: in-group bonding versus no-bonding control) × 2 (role: attacker versus defender) mixed-model ANOVA with significant effects thresholded at $P < 0.05$, FDR corrected for multiple comparisons of all 14 channels (see Supplementary Table 5 for the full statistical reports). The F and T maps were smoothed using the spline method.

Next, we examined the link between neural synchronization and behavioral group decisions by correlating group contribution with GNS. We observed opposite relationships between group contribution and GNS in attackers (positive correlation) and defenders (negative correlation). Thus, to test whether the group role modulated the association between GNS and group contribution (GC), we treated attacker and defender groups as separate three-person sessions and investigated whether the GNS–GC relationship differed between attacker and defender groups. We correlated the within-group neural synchronization (GNS$_i$) with group contribution (GC$_i$) for attacker and defender groups, respectively. We then transformed and compared the coefficients (r_A for attacker and r_D for defender) using two-tailed Fisher r-to-z transformation (http://vassarstats.net/rdiff.html). The calculation of the z value was used to assess the significance of the differences between the two coefficients. If r_A is significantly different from r_D, the relationship between GNS and GC is conditioned by group role.

Given that neural synchronization mainly reflects the phase-locked relationship between two neural signals[69], it provides insight into how socially shared representations and understanding are built[49]. However, we cannot tell whether synchronized neural signals were increased or decreased by the task[73]. We thus analyzed within-individual neural activity to further understand the functionality of neural activity and its synchronization during intergroup conflicts. Regarding individual neural activity (Extended Data Fig. 5a), we first performed pre-processing on the fNIRS de-noised oxy-Hb data using MATLAB-based functions derived from the NIRS-SPM toolbox. Discrete cosine transforms with a cutoff period of 128 s and pre-coloring based on hemodynamic response function were applied to the de-noised oxy-Hb data to remove longitudinal

signal drift, motion artifacts and respiration and cardiac oscillations from the signal. The pre-processed oxy-Hb time series of each channel were segmented into three conditions, similar to the neural synchronizaton analysis (i.e. the group decision-making phase, the waiting screen phase and the outcome screen phase). The decision-making phase (outcome-processing phase) related activation was considered as increases in oxy-Hb during the group decision-making phase (outcome screen phase) in contrast to the waiting screen phase, after a z-score transformation using the mean value and standard deviation of the waiting phase[74]. For each intergroup contest round, we averaged across three participants sharing the same role to indicate the within-group averaged, round-level neural responses of each three-person group. We first averaged the group neural responses across all contest rounds and submitted them to bonding-by-role ANOVA. Moreover, at the round level, for each three-person group, we examined whether the within-group averaged neural responses to the outcome of a current round could guide the three-person group's average contribution on the next round. We built a linear regression of GC on round T (GC$_T$, with T ranging from 2 to 24) as a function of within-group averaged rDLPFC activity on the last round T-1 (round 1–23; with the standardized coefficient of the regression β indicating the prediction strength) for each three-person group. The Fisher z-transformed β across conditions was compared against 0 to examine whether the neural response could indeed predict group contribution decisions. In addition, we performed coherence analyses between rTPJ and rDLPFC for each individual (Extended Data Fig. 5b). We then averaged the coherence values across the three participants within the same group to index group-averaged functional connectivity (GFC) of rDLPFC–rTPJ. We then submitted this rDLPFC–rTPJ GFC index to bonding-by-role ANOVA at the channel-pairwise level (each of the seven channels in the rDLPFC with each of the seven channels in the rTPJ, i.e. 49 channel pairs) and at the grand mean level (i.e. the averaged coherence value of 49 channel pairs).

Identification of significant effects. We applied FDR correction[75] to correct for the number of simultaneously conducted tests to control for type I errors[76,77] and focused on the channels of interest when analyses were performed to further decompose the effect to control for type II errors. Specifically, our primary research question focused on within-group neural synchronization and asked whether and how the in-group bonding and group role modulated GNS. Similar to previous studies[18,69], we applied FDR correction to channel-wise analysis (i.e. corrected for all 14 channels) when looking at the effects of bonding and/or role on GNS. The bonding × role interaction was reliable after 14-channel-wise FDR correction at channels 8 and 11 in the rDLPFC and at channels 4 and 13 in the rTPJ. Then, we conducted correlation analyses (between GNS and group contributions) at the channels in which GNS was modulated by role and/or bonding (i.e. channels 8, 11, 4 and 13) to further link GNS with group behavior. The relationship between GNS and group contribution was found in the rDLPFC channels, and only channel 8 survived FDR correction for testing channels.

Analyses on group-averaged activity were conducted to further understand the interaction effects on neural synchronization and to reveal whether neural activity was synchronized in an increasing or decreasing manner. Thus, similar to previous studies[74,78] and to control for type II errors[79], we narrowed our focus to the channel of interest that exhibited significant effects of role and/or bonding on GNS and in predicting group contribution (i.e. channel 8). Finally, for the rDLPFC–rTPJ connectivity, we did not have a prior hypothesis about the effect of role or bonding on the functional connectivity. We thus performed FDR correction for all 49 channel pairs and identified significant effects only if surviving from 49 multiple comparisons.

Additional analyses and results. To validate the effect that we observed of bonding and/or role on GNS in the real interacting groups, we generated within-condition pseudo groups by randomly grouping three individuals from different original real groups under the same condition as a pseudo group (Extended Data Fig. 2c). To test whether the bonding × role interaction on GNS was specific to real interacting groups, we conducted role (attacker versus defender) × bonding (in-group bonding versus no-bonding control) × Group (real versus pseudo groups) ANOVA on GNS during decision-making in the channels that showed significant bonding × role interaction in real groups (Extended Data Fig. 3a). To further verify the stronger bonding-by-role interaction effect on GNS in real interacting groups than in pseudo groups, we conducted permutation tests, which is a nonparametric statistical significance testing approach that tests the null hypothesis of no difference between real groups and pseudo groups. We tested the observed bonding-by-role interactive effects on GNS of the real group against the permutation samples based on the bonding-by-role interactive effects on GNS ($n = 1,000$, each permutation sample contained 172 within-condition pseudo groups)[18,68,80]. This analysis confirmed that the observed interactive effects on GNS in real groups were outside the 95% CI of the permutation distribution of the 1,000 pseudo-group samples with significant empirical P values (channel 8: $P < 0.001$; channel 11: $P < 0.001$; channel 4: $P = 0.015$; channel 13: $P = 0.001$, survived FDR correction for the testing channels, Extended Data Fig. 3b).

To present measured neural synchronization from different perspectives, the results based on deoxy-Hb signals were also analyzed. We employed the same wavelet transform coherence analysis to calculate the GNS of each three-person

group. Previous studies showed that the oxy-Hb signal has a higher signal-to-noise ratio than the deoxy-Hb signal[81,82] and is a more sensitive indicator of changes in regional cerebral blood flow[67,69,83]. The deoxy-Hb signal is, in contrast, more related to neurovascular coupling[84]. We reported the results based on oxy-Hb signal in the main text and the results based on deoxy-Hb signals in Supplementary Fig. 2.

To examine the effect of bonding over time, we included time-bin as an independent factor in ANOVA on GNS. Specifically, we clustered the 24 rounds into four time-bins (i.e. six contest rounds per bin) and averaged GNS for each time-bin. We then submitted the averaged GNS of each time-bin to role (attacker versus defender) × bonding (in-group bonding versus no-bonding control) × time-bin mixed-model ANOVA. Although the bonding × role interaction on GNS remained significant, we did not find a significant main effect of time-bin or an interaction between time-bin and role and/or bonding, suggesting that the effects of bonding and role reported in the main text were stable across time.

In each six-person session, all six participants were of the same gender. To examine the role of session gender, we included Session gender (all-male versus all-female sessions) as a between-sessions factor in all models reported in the main text. Session gender produced a main effect, with stronger GNS in the rDLPFC (channels 6 and 8) and rTPJ (channel 13) in all-female sessions than in all-male sessions (Supplementary Fig. 3a and Supplementary Table 10a), but Session gender did not interact with in-group bonding or group role (Supplementary Table 10a). We did not observe a main effect of Session gender or its interaction with in-group bonding or group role on within-group averaged neural activity (Supplementary Fig. 3b and Supplementary Table 10b) or group-averaged functional connectivity (Supplementary Fig. 3c and Supplementary Table 10c). We concluded from these analyses that our main findings and conclusions generalize across all-male and all-female intergroup contests.

In addition, we conducted an alternative analysis on group-level neural activity and functional connectivity, which enabled comparisons between real and pseudo groups. Different from the group-averaged (individual) neural activity and functional connectivity, we performed grouping from the first step by averaging the raw de-noised oxy-Hb time series (a group-level raw time series) and then calculated neural activity and functional connectivity based on the group-level oxy-Hb time series (Extended Data Fig. 10). This analysis showed the similar bonding effect on group-level neural activity (Supplementary Fig. 4) and functional connectivity (Supplementary Fig. 5 and Supplementary Table 11) as that in the analysis of group-averaged (individual) level.

Statistics. Sample size estimation was performed a priori. The role (attacker versus defender) was randomly assigned and blinded to the experimenter during data collection. Data analysis was not performed blinded to the conditions of the experiment. Both behavioral and neural data were first aggregated at the three-person group level and submitted to two-way mixed-model ANOVA with role (attacker versus defender) as a within-subjects factor and bonding (in-group bonding versus no-bonding control) as a between-subjects factor. ANOVA with significant interaction were followed by planned two-tailed t-tests to examine: (1) the effect of role (two-tailed paired-samples t-test) separately in groups under the in-group bonding and no-bonding control and (2) the effect of bonding (two-tailed independent-samples t-test) separately for attacker and defender groups. Data distribution was assumed to be normal, but this was not formally tested. Correlations were performed by Pearson's correlation coefficient analysis. FDR correction was applied whenever multiple tests were conducted.

Reporting Summary. Further information on research design is available in the Nature Research Reporting Summary linked to this article.

Data availability

All behavioral data and materials have been made publicly available via the Open Science Framework and can be accessed at https://osf.io/uh3sx/. The neural data that support the findings of this study are available from the corresponding author upon reasonable request.

Code availability

The custom routines for data analysis written in MATLAB are available from the corresponding author upon reasonable request.

References

50. Faul, F., Erdfelder, E., Buchner, A. & Lang, A. G. Statistical power analyses using G* Power 3.1: tests for correlation and regression analyses. *Behav. Res. Methods* **41**, 1149–1160 (2009).
51. Duan, L. et al. Cluster imaging of multi-brain networks (CIMBN): a general framework for hyperscanning and modeling a group of interacting brains. *Front. Neurosci.* **9**, 267 (2015).
52. Nozawa, T., Sasaki, Y., Sakaki, K., Yokoyama, R. & Kawashima, R. Interpersonal frontopolar neural synchronization in group communication: an exploration toward fNIRS hyperscanning of natural interactions. *Neuroimage* **133**, 484–497 (2016).
53. Balliet, D., Wu, J. & De Dreu, C. K. Ingroup favoritism in cooperation: a meta-analysis. *Psychol. Bull.* **140**, 1556–1581 (2014).
54. Liebe, U. & Tutic, A. Status groups and altruistic behaviour in dictator games. *Ration. Soc.* **22**, 353–380 (2010).
55. Gaertner, L. & Schopler, J. Perceived ingroup entitativity and intergroup bias: an interconnection of self and others. *Eur. J. Soc. Psychol.* **28**, 963–980 (1998).
56. Ensari, N. & Miller, N. Decategorization and the reduction of bias in the crossed categorization paradigm. *Eur. J. Soc. Psychol.* **31**, 193–216 (2001).
57. Osaka, N., Minamoto, T., Yaoi, K., Azuma, M., Shimada, Y. M. & Osaka, M. How two brains make one synchronized mind in the inferior frontal cortex: fNIRS-based hyperscanning during cooperative singing. *Front. Psychol.* **6**, 1811–1821 (2015).
58. Koessler, L. et al. Automated cortical projection of EEG sensors: anatomical correlation via the international 10–10 system. *Neuroimage* **46**, 64–72 (2009).
59. Lu, K., Xue, H., Nozawa, T. & Hao, N. Cooperation makes a group be more creative. *Cereb. Cortex* **22**, 1–14 (2018).
60. Obrig, H. & Villringer, A. Beyond the visible—imaging the human brain with light. *J. Cereb. Blood Flow Metab.* **23**, 1–18 (2003).
61. Hoshi, Y. Functional near-infrared spectroscopy: current status and future prospects. *J. Biomed. Opt.* **12**, 062106 (2007).
62. Huppert, T. J., Hoge, R. D., Diamond, S. G., Franceschini, M. A. & Boas, D. A. A temporal comparison of BOLD, ASL, and NIRS hemodynamic responses to motor stimuli in adult humans. *Neuroimage* **29**, 368–382 (2006).
63. Cui, X., Bray, S., Bryant, D. M., Glover, G. H. & Reiss, A. L. A quantitative comparison of NIRS and fMRI across multiple cognitive tasks. *Neuroimage* **54**, 2808–2821 (2011).
64. Strangman, G., Culver, J. P., Thompson, J. H. & Boas, D.A. A quantitative comparison of simultaneous BOLD fMRI and NIRS recordings during functional brain activation. *Neuroimage* **17**, 719–731 (2002).
65. Duan, L. et al. Wavelet-based method for removing global physiological noise in functional near-infrared spectroscopy. *Biomed. Opt. Express* **9**, 3805–3820 (2018).
66. Jang, K. E. et al. Wavelet minimum description length detrending for near-infrared spectroscopy. *J. Biomed. Opt.* **14**, 034004 (2009).
67. Molavi, B. & Dumont, G. A. Wavelet-based motion artifact removal for functional near-infrared spectroscopy. *Physiol. Meas.* **33**, 259–270 (2012).
68. Liu, W. et al. Shared neural representations of syntax during online dyadic communication. *Neuroimage* **198**, 63–72 (2019).
69. Cui, X., Bryant, D. M. & Reiss, A. L. NIRS-based hyperscanning reveals increased interpersonal coherence in superior frontal cortex during cooperation. *Neuroimage* **59**, 2430–2437 (2012).
70. Torrence, C. & Compo, G. P. A practical guide to wavelet analysis. *Bull. Am. Meteorol. Soc* **.79**, 61–78 (1998).
71. Hu, Y., Hu, Y., Li, X., Pan, Y. & Cheng, X. Brain-to-brain synchronization across two persons predicts mutual prosociality. *Soc. Cogn. Affect. Neurosci.* **12**, 1835–1844 (2017).
72. Xue, H., Lu, K. & Hao, N. Cooperation makes two less-creative individuals turn into a highly-creative pair. *Neuroimage* **172**, 527–537 (2018).
73. Baker, J. M. et al. Sex differences in neural and behavioral signatures of cooperation revealed by fNIRS hyperscanning. *Sci. Rep* **6**, 26492 (2016).
74. Liu, T., Saito, G., Lin, C. & Saito, H. Inter-brain network underlying turn-based cooperation and competition: a hyperscanning study using near-infrared spectroscopy. *Sci. Rep.* **7**, 8684–8695 (2017).
75. Benjamini, Y. & Hochberg, Y. Controlling the false discovery rate: a practical and powerful approach to multiple testing. *J. R. Stat. Soc. Series B Methodol.* **57**, 289–300 (1995).
76. Singh, A. K. & Dan, I. Exploring the false discovery rate in multichannel NIRS. *Neuroimage* **33**, 542–549 (2006).
77. Tak, S. & Ye, J. C. Statistical analysis of fNIRS data: a comprehensive review. *Neuroimage* **85**, 72–91 (2014).
78. Hampshire, A., Chamberlain, S. R., Monti, M. M., Duncan, J. & Owen, A. M. The role of the right inferior frontal gyrus: inhibition and attentional control. *Neuroimage* **50**, 1313–1319 (2010).
79. Poldrack, R. A. Region of interest analysis for fMRI. *Soc. Cogn. Affect. Neurosci.* **2**, 67–70 (2007).
80. Bilek, E. et al. Information flow between interacting human brains: identification, validation, and relationship to social expertise. *Proc. Natl Acad. Sci. U.S.A* **112**, 5207–5212 (2015).
81. Ding, X. P., Sai, L., Fu, G., Liu, J. & Lee, K. Neural correlates of second-order verbal deception: a functional near-infrared spectroscopy (fNIRS) study. *Neuroimage* **87**, 505–514 (2014).
82. Taga, G., Asakawa, K., Maki, A., Konishi, Y. & Koizumi, H. Brain imaging in awake infants by near-infrared optical topography. *Proc. Natl Acad. Sci. USA* **100**, 10722–10727 (2003).
83. Tachtsidis, I. & Scholkmann, F. False positives and false negatives in functional near-infrared spectroscopy: issues, challenges, and the way forward. *Neurophotonics* **3**, 031405 (2016).

84. Ou, W. et al. Study of neurovascular coupling in humans via simultaneous magnetoencephalography and diffuse optical imaging acquisition. *Neuroimage* **46**, 624–632 (2009).

Author contributions

Y.M. and C.K.W.D.D. conceived of the project. J.Y., H.Z., C.K.W.D.D and Y.M. designed the experiments. J.Y., H.Z. and J.N. implemented the experiment and collected data. J.Y. and H.Z. pre-processed the data and performed analyses. All authors discussed results. J.Y., H.Z., C.K.W.D.D. and Y.M. wrote the paper.

Competing interests

The authors declare no competing interests.

Additional information

Extended data is available for this paper at https://doi.org/10.1038/s41593-020-0630-x.

Supplementary information is available for this paper at https://doi.org/10.1038/s41593-020-0630-x.

Correspondence and requests for materials should be addressed to Y.M.

**Reprints and permissions information** is available at www.nature.com/reprints.
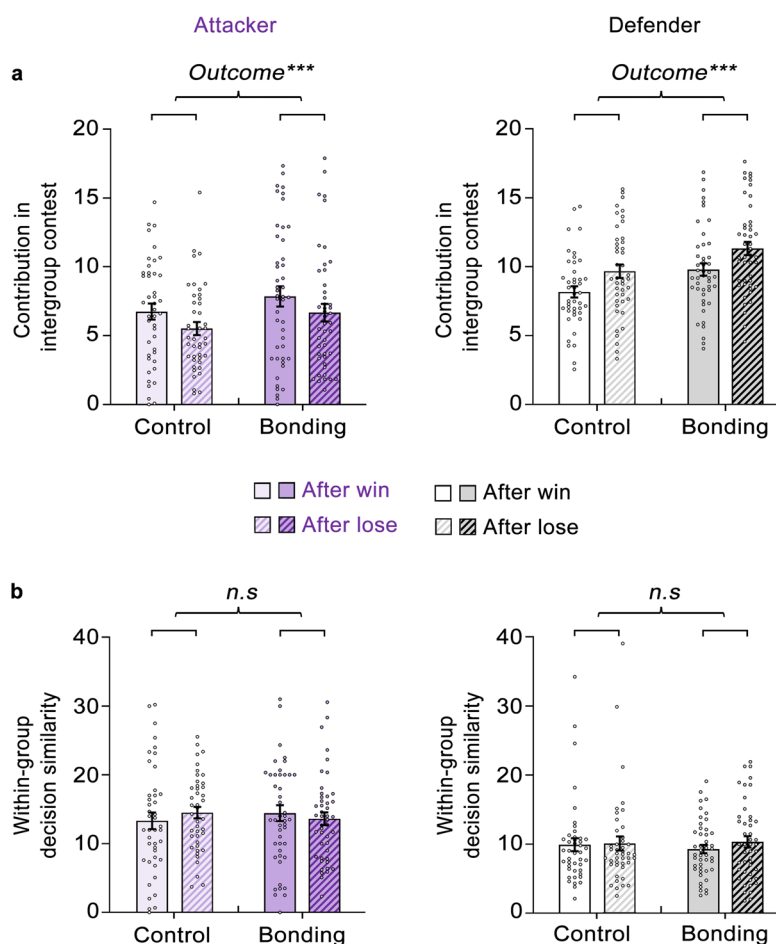
Extended Data Fig. 1 | The Effects of Winning or Losing a Contest Round on Behavioral Measures. We examined how the contest outcome (win or lose the contest) influenced group members' behaviors, respectively for attacker and defender groups. **a**, We found that, after losing the last round, attackers decreased their contribution to group fighting ($F_{1,87} = 22.336$, $p = 8.74 \times 10^{-6}$, $\eta^2 = 0.204$) whereas defenders increased their contribution ($F_{1,87} = 77.894$, $p = 1.02 \times 10^{-13}$, $\eta^2 = 0.472$). The effect of Outcome was not affected by the bonding conditions (utcome-by-Bonding interaction, attacker: $F_{1,87} = 0.013$, $p = 0.911$, $\eta^2 = 1.44 \times 10^{-4}$; defender: $F_{1,87} = 0.007$, $p = 0.936$, $\eta^2 = 7.52 \times 10^{-5}$). **b**, Outcome did not influence within-group decision similarity (main effect of Outcome, attacker: $F_{1,87} = 0.074$, $p = 0.786$, $\eta^2 = 0.001$; defender: $F_{1,87} = 2.860$, $p = 0.094$, $\eta^2 = 0.032$; Outcome-by-Bonding interaction, attacker: $F_{1,87} = 2.055$, $p = 0.155$, $\eta^2 = 0.023$; defender: $F_{1,87} = 1.265$, $p = 0.264$, $\eta^2 = 0.014$). Data from two sessions were excluded as attackers in these two sessions did not win any of the 24 rounds. Outcome-by-Bonding mixed-model ANOVAs ($n = 89$, 43 three-person groups under no-bonding control and 46 three-person groups under in-group bonding separately for attacker groups and defender groups). Data showed as Mean ± S.E. with overlaid dot plots. ***$p < 0.001$, *n.s.* not significant. Note: Given the limited and unequal number of after-win and after-lose rounds, we calculated another index to indicate group decision coordination, i.e., within-group decision similarity. For each 3-person group, we calculated the within-group decision similarity as the investment difference of each pair of the 3-person group for each round [i.e., ($|x_1 - x_2| + |x_2 - x_3| + |x_1 - x_3|$) for attacker group; ($|y_1 - y_2| + |y_2 - y_3| + |y_1 - y_3|$) for defender group].
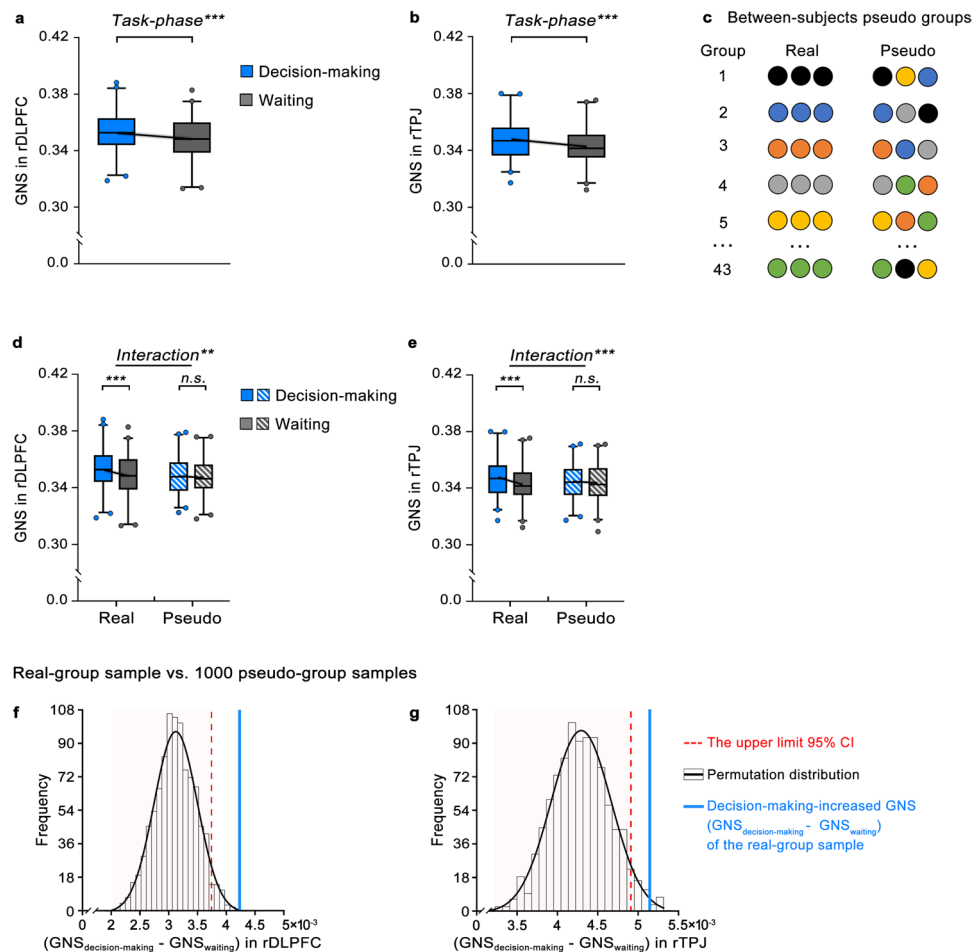
Extended Data Fig. 2 | Increased Within-group Neural Synchronization during Decision-making Phase relative to Waiting Phase. We compared within-group neural synchronization (GNS) during the group decision-making phase with that during the waiting screen of the intergroup contest game. **a**,**b**, We averaged GNS across the channels located in the rDLPFC and rTPJ respectively, and showed higher GNS during decision-making than waiting phases (**a**, rDLPFC: $t_{85} = 5.823$, $p = 1.00 \times 10^{-7}$, Cohen's $d = 0.628$, 95% CI = 0.003, 0.006, **b**, rTPJ: $t_{85} = 6.578$, $p = 3.70 \times 10^{-9}$, Cohen's $d = 0.709$, 95% CI = 0.004, 0.007), indicating increased GNS during group decision-making. Two-tailed paired samples t-tests, 86 six-person groups during decision-making and during waiting phases. **c**, To validate the Phase effect on the GNS, we generated within-condition pseudo groups for comparison purpose by randomly grouping 3 individuals from different original real groups under the same condition as a pseudo group, and treated Group (real vs. pseudo groups) as a between-subjects factor. **d**,**e**, We conducted ANOVAs on GNS with factors of Phase (decision-making vs. waiting) and Group (real vs. pseudo groups) in 86 six-person real groups and 86 six-person pseudo groups. We observed significant Phase-by-Group interactions on GNS in rDLPFC and rTPJ (**d**, rDLPFC: $F_{1,170} = 10.161$, $p = 0.002$, $\eta^2 = 0.056$; **e**, rTPJ: $F_{1,170} = 13.920$, $p = 2.60 \times 10^{-4}$, $\eta^2 = 0.076$). In addition, two-tailed paired t-tests on 86 six-person pseudo groups showed no significant difference between GNS during decision-making and waiting phases (**d**, rDLPFC: $t_{85} = 1.400$, $p = 0.165$, Cohen's $d = 0.151$, 95% CI = -4.16×10^{-4}, 0.002; **e**, rTPJ: $t_{85} = 1.209$, $p = 0.230$, Cohen's $d = 0.130$, 95% CI = -0.001, 0.003). Data are plotted as boxplots for each condition in which horizontal lines indicate median values, boxes indicate 25/75% quartiles, and whiskers indicate the 2.5-97.5% percentile range. Data points outside the range are shown separately as circles. Solid lines start from the mean and reflect the intervals for the Mean ± S.E. **$p < 0.01$, ***$p < 0.001$, n.s. not significant. **f**, **g**, One-sided permutation test was used to verify the stronger decision-making-increased GNS in real than pseudo groups. Specifically, we calculated the mean difference between the two phases (GNS$_{decision-making}$ – GNS$_{waiting}$) to indicate decision-making-increased GNS respectively for each real or pseudo group. We then compared the real-group sample with 1000 pseudo-group samples[18,68,80]. We tested the decision-making-increased GNS of the real sample against permutation samples based on decision-making-increased GNS ($n = 1000$, each permutation sample contains 172 within-condition 3-person pseudo groups). To test whether the effects observed in real groups was larger than that in pseudo groups, we reported the 1-sided p-values. The empirical p value was calculated as[80]: $p = j/1000$, j is the number of samples out of the 1000 permutation samples, of which the decision-making-increased GNS was larger than the observed value of real groups. We showed that, for both rDLPFC and rTPJ, the observed difference in decision-making-increased GNS in real groups were outside the upper limit of 95% CI of the permutation distribution. The one-sided p-values indicated specific decision-making-increased GNS in real groups rather than pseudo groups (f, rDLPFC: $p = 0.004$; g, rTPJ: $p = 0.012$).
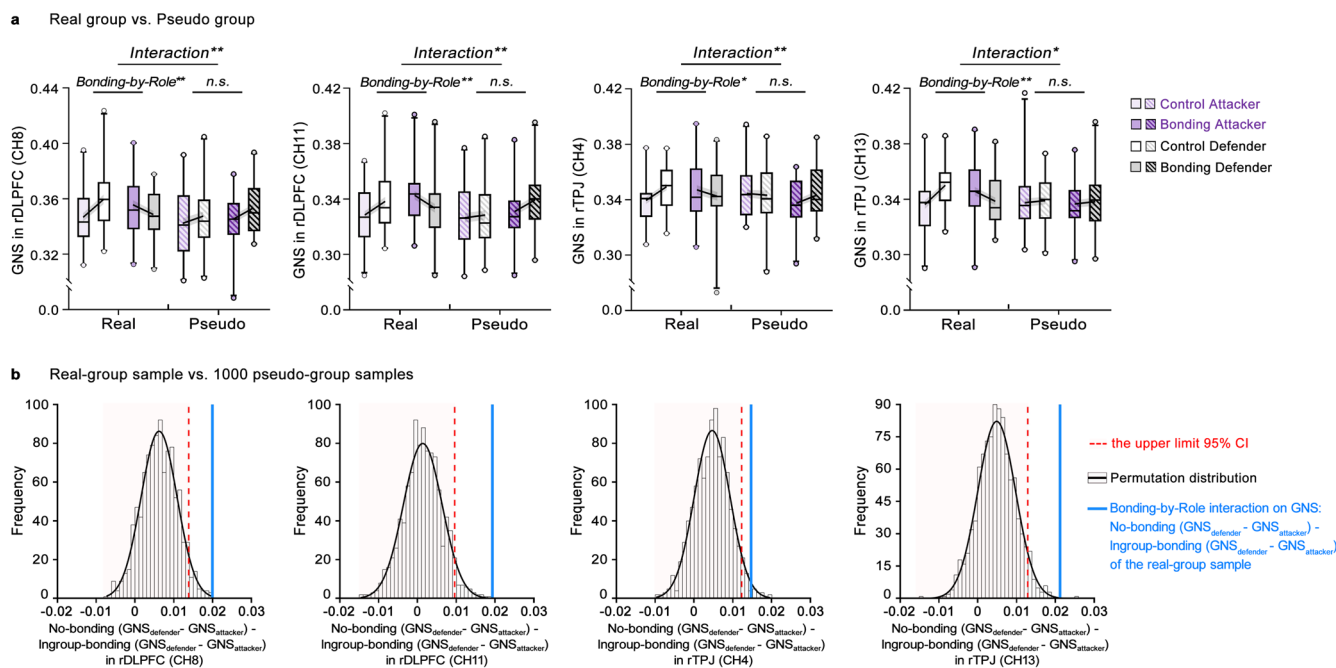
Extended Data Fig. 3 | Validation of Bonding-by-Role interaction on Within-group Neural Synchronization. a, To confirm stronger Bonding-by-Role interaction in real than pseudo groups, we conducted 3-way ANOVAs on GNS with factors of Bonding, Role, and Group, at channels that showed significant Bonding-by-Role interaction in real groups (86 six-person real groups and 86 six-person pseudo groups). We observed significant 3-way interaction of Bonding-by-Role-by-Group on GNS in rDLPFC and TPJ (channel 8: $F_{1,168} = 7.578$, $p = 0.007$, $\eta^2 = 0.043$; channel 11: $F_{1,168} = 8.318$, $p = 0.004$, $\eta^2 = 0.047$; channel 4: $F_{1,168} = 7.085$, $p = 0.009$, $\eta^2 = 0.040$; channel 13: $F_{1,168} = 5.111$, $p = 0.025$, $\eta^2 = 0.030$, survived FDR correction for the testing channels). Bonding-by-Role interaction in pseudo groups were not significant (channel 8: $F_{1,84} = 0.292$, $p = 0.590$, $\eta^2 = 0.003$; channel 11: $F_{1,84} = 1.096$, $p = 0.298$, $\eta^2 = 0.013$; channel 4: $F_{1,84} = 1.424$, $p = 0.236$, $\eta^2 = 0.017$; channel 13: $F_{1,84} = 0.016$, $p = 0.900$, $\eta^2 = -1.88 \times 10^{-4}$). Data are plotted as boxplots for each condition in which horizontal lines indicate median values, boxes indicate 25/75% quartiles, and whiskers indicate the 2.5-97.5% percentile range. Data points outside the range are shown separately as circles. Solid lines start from the mean and reflect the intervals for the Mean $\pm$ S.E. $*p < 0.05$, $**p < 0.01$, n.s. not significant. **b**, One-sided permutation test was conducted to verify the stronger Bonding-by-Role on GNS in real than pseudo groups. Specifically, we compared the real-group sample with 1000 pseudo-group samples[18,68,80]. We calculated the Bonding-by-Role interaction on GNS: No-bonding ($GNS_{defender} - GNS_{attacker}$) – Ingroup-bonding ($GNS_{defender} - GNS_{attacker}$), for each real and pseudo group. We then tested the observed Bonding-by-Role interactive effects on GNS of the real groups against the permutation samples based on the Bonding-by-Role interactive effects on GNS ($n = 1000$, each permutation sample contains 172 within-condition three-person pseudo groups). We showed that the observed differences in the interactive effects on GNS in real groups were outside the upper limit of 95% CI of the permutation distribution. The empirical p value was calculated as[80]: $p = j/1000$, j is the number of samples out of the 1000 permutation samples, of which the Bonding-by-Role interaction on GNS was larger than the observed value of real groups. The one-sided p-values indicated stronger interaction on GNS in real groups (channel 8: $j = 0$; channel 11: $j = 0$; channel 4: $p = 0.015$; channel 13: $p = 0.001$, survived FDR-correction for the testing channels).
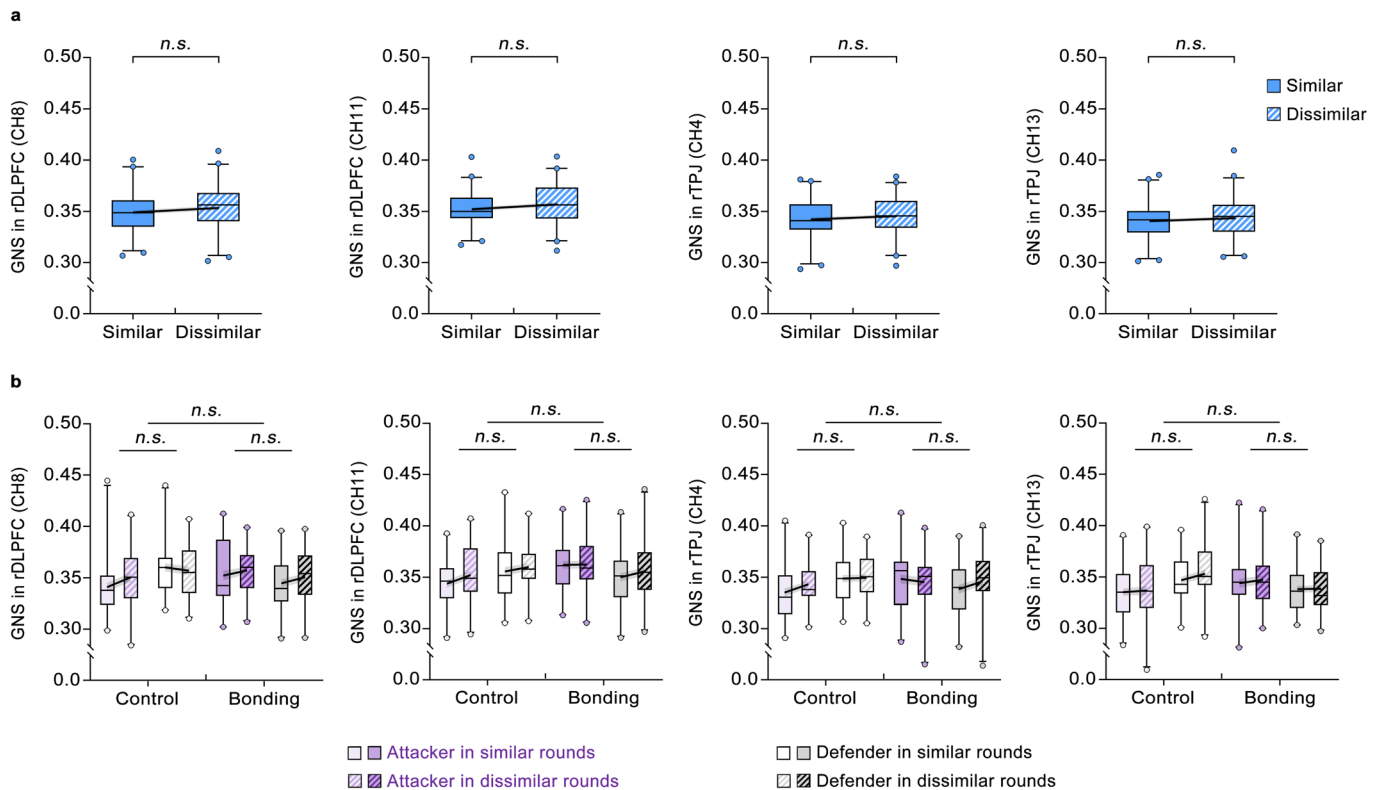
Extended Data Fig. 4 | The Effect of Decision Similarity on Within-group Neural Synchronization (GNS). To test whether GNS just reflected individual making similar decisions, we included a within-subject factor (within-group decision similarity) in the analyses, resulting in Role (attacker vs. defender) × Bonding (in-group bonding vs. control) × Similarity (similar vs. dissimilar) mixed-model ANOVAs on GNS. For each 3-person group, each contest round, we calculated the within-group decision similarity as the investment difference of each pair of the 3-person group for each round [i.e., $(|x_1 - x_2| + |x_2 - x_3| + |x_1 - x_3|)$ for attacker group; $(|y_1 - y_2| + |y_2 - y_3| + |y_1 - y_3|)$ for defender group]. Using median split on the mean value of decision similarity across all rounds, we categorized all the rounds into "similar" and "dissimilar" decisions. First, the Bonding × Role interaction remained significant when including within-group decision similarity in the analysis in rDLPFC. However, the main effect of Similarity (**a**, channel 8: $F_{1,84} = 2.334$, $p = 0.130$, $\eta^2 = 0.027$; channel 11: $F_{1,84} = 3.553$, $p = 0.063$, $\eta^2 = 0.041$; channel 4: $F_{1,84} = 1.568$, $p = 0.214$, $\eta^2 = 0.018$; channel 13: $F_{1,84} = 1.203$, $p = 0.276$, $\eta^2 = 0.014$) or its interaction with Role and/or Bonding (**b**, Similarity-by-Role-by-Bonding: channel 8: $F_{1,84} = 2.019$, $p = 0.159$, $\eta^2 = 0.023$; channel 11: $F_{1,84} = 1.191$, $p = 0.278$, $\eta^2 = 0.014$, channel 4: $F_{1,84} = 3.627$, $p = 0.060$, $\eta^2 = 0.041$; channel 13: $F_{1,84} = 0.579$, $p = 0.449$, $\eta^2 = 0.007$; Similarity-by-Role: channel 8: $F_{1,84} = 1.445$, $p = 0.233$, $\eta^2 = 0.017$; channel 11: $F_{1,84} = 0.016$, $p = 0.899$, $\eta^2 = 1.94 \times 10^{-4}$, channel 4: $F_{1,84} = 0.126$, $p = 0.724$, $\eta^2 = 0.001$; channel 13: $F_{1,84} = 0.026$, $p = 0.873$, $\eta^2 = 3.07 \times 10^{-4}$; Similarity-by-Bonding: channel 8: $F_{1,84} = 0.157$, $p = 0.693$, $\eta^2 = 0.002$; channel 11: $F_{1,84} = 0.473$, $p = 0.493$, $\eta^2 = 0.006$, channel 4: $F_{1,84} = 0.172$, $p = 0.679$, $\eta^2 = 0.002$; channel 13: $F_{1,84} = 0.160$, $p = 0.690$, $\eta^2 = 0.002$) did not reach significance. Mixed-model ANOVAs, $n = 86$ three-versus-three-person intergroup competitions. Data are plotted as boxplots for each condition in which horizontal lines indicate median values, boxes indicate 25% and 75% quartiles, and whiskers indicate the 2.5-97.5% percentile range. Data points outside the range are shown separately as circles. Solid lines start from the mean and reflect the intervals for the Mean ± S.E. *n.s.* not significant.
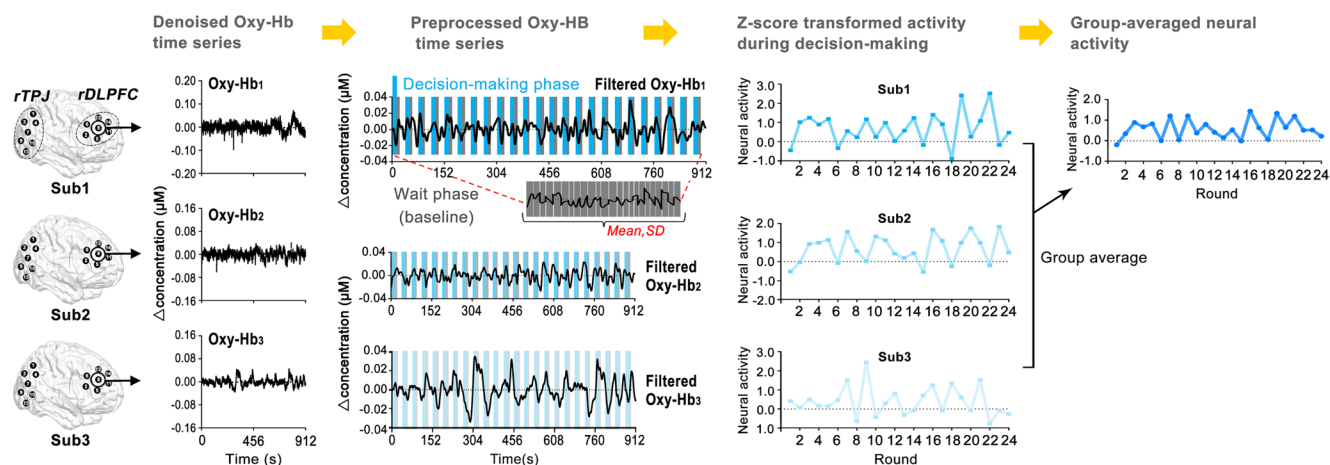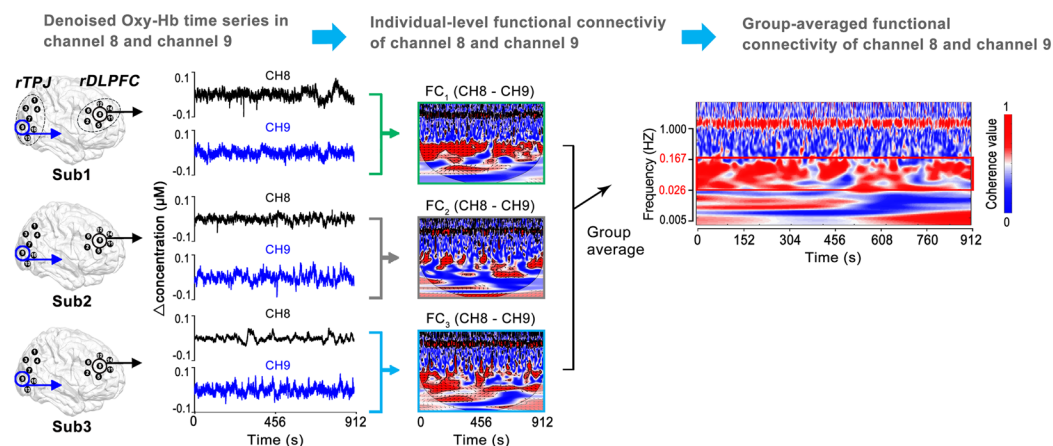
Extended Data Fig. 5 | Illustration of Group-averaged Neural Activity and rDLPFC-rTPJ Connectivity Analyses. a, *Group-averaged Neural Activity*. We first assessed the neural responses of a single brain (i.e., individual neural activity) by performing pre-processing on the fNIRS denoised Oxy-Hb data, including discrete cosine transforms with cut-off period of 128 s and pre-coloring based on hemodynamic response function (HRF). The preprocessed Oxy-Hb time series of each channel were segmented into 3 conditions, i.e., the decision-making phase (illustrated in the figure), the waiting screen, and the outcome screen. The pre-processed Oxy-Hb during decision-making (outcome) phase was z-score transformed using the mean value and standard deviation of the waiting period (as baseline) and indicated decision-making (outcome) related activity[74]. For each intergroup contest, we averaged across 3 participants sharing the same role to indicate the round-level neural responses of each 3-person group. **b**, *Group-averaged rDLPFC-rTPJ connectivity*. Similar to previous studies[37], we performed coherence analysis between each of the 7 channels in the rDLPFC with each of the 7 channels in the rTPJ (i.e., 49 channel pairs) for each participant. The calculation of functional connectivity between channel 8 in the rDLPFC and channel 9 in the rTPJ was illustrated in the figure. We then averaged the coherence values of the 3 participants within the same group to indicate the group-averaged functional connectivity (GFC) of rDLPFC–rTPJ.
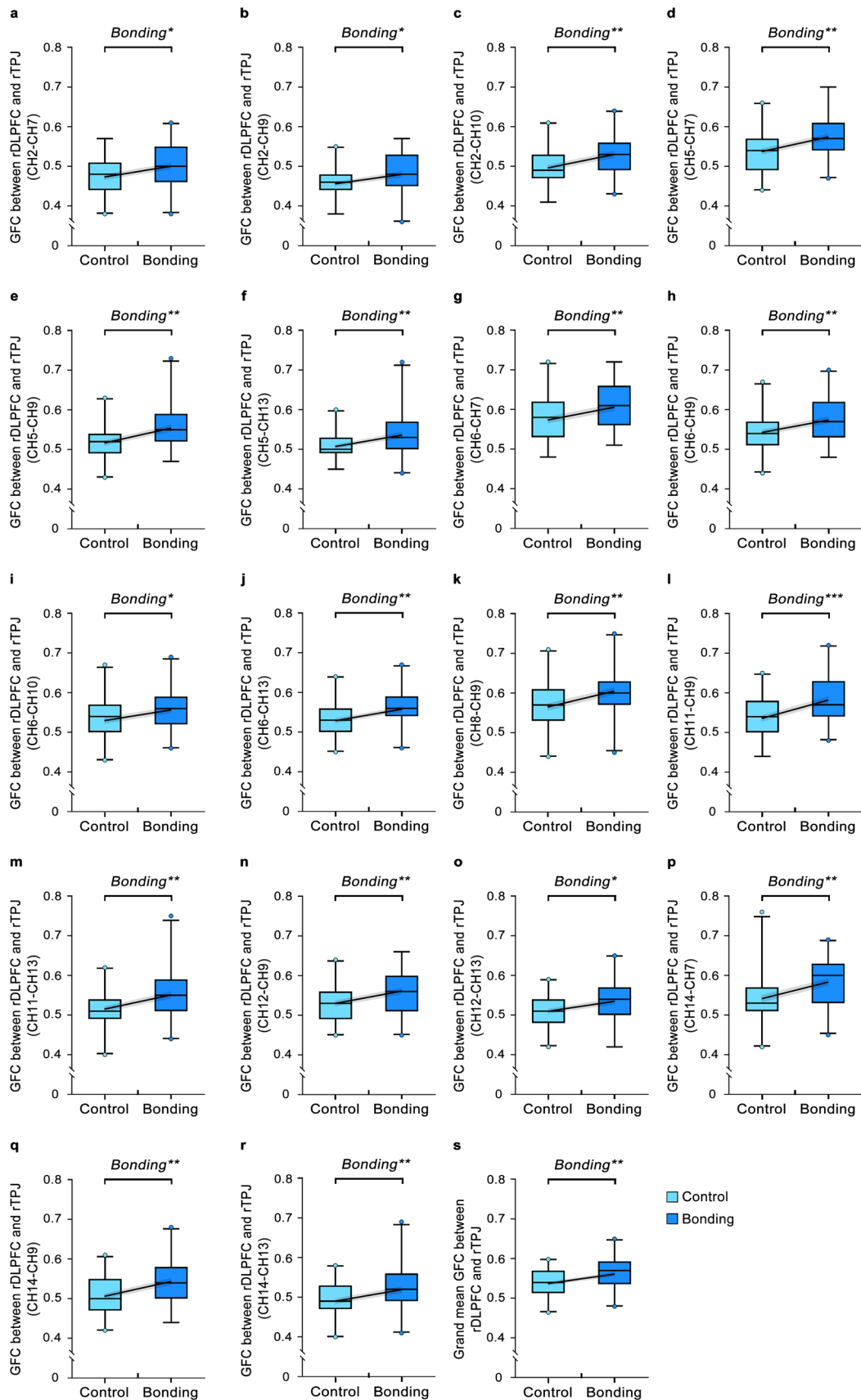
**Extended Data Fig. 6 | See next page for caption.**

Extended Data Fig. 6 | In-group Bonding Increased Group-averaged Functional Connectivity (GFC) of rDLPFC-rTPJ. We conducted Bonding (in-group bonding vs. no-bonding control) × Role (attacker vs. defender) mixed-model ANOVAs on the GFC of rDLPFC-rTPJ. We showed that in-group bonding (relative to no-bonding control) increased rDLPFC-rTPJ connectivity in 18 rDLPFC-rTPJ channel pairs (FDR corrected for 49 rDLPFC-rTPJ channel pairs, **a–r**, Supplementary Table 8 gives the full statistical report) and grand mean rDLPFC-rTPJ connectivity (**s**, $F_{1,84} = 9.033$, $p = 0.003$, $\eta^2 = 0.097$). Mixed-model ANOVAs, $n = 86$ three-versus-three-person intergroup competitions. Data are plotted as boxplots for each condition in which horizontal lines indicate median values, boxes indicate 25/75% quartiles, and whiskers indicate the 2.5-97.5% percentile range. Data points outside the range are shown separately as circles. Solid lines start from the mean and reflect the intervals for the Mean ± S.E. *$p<0.05$, **$p<0.01$, ***$p<0.001$.
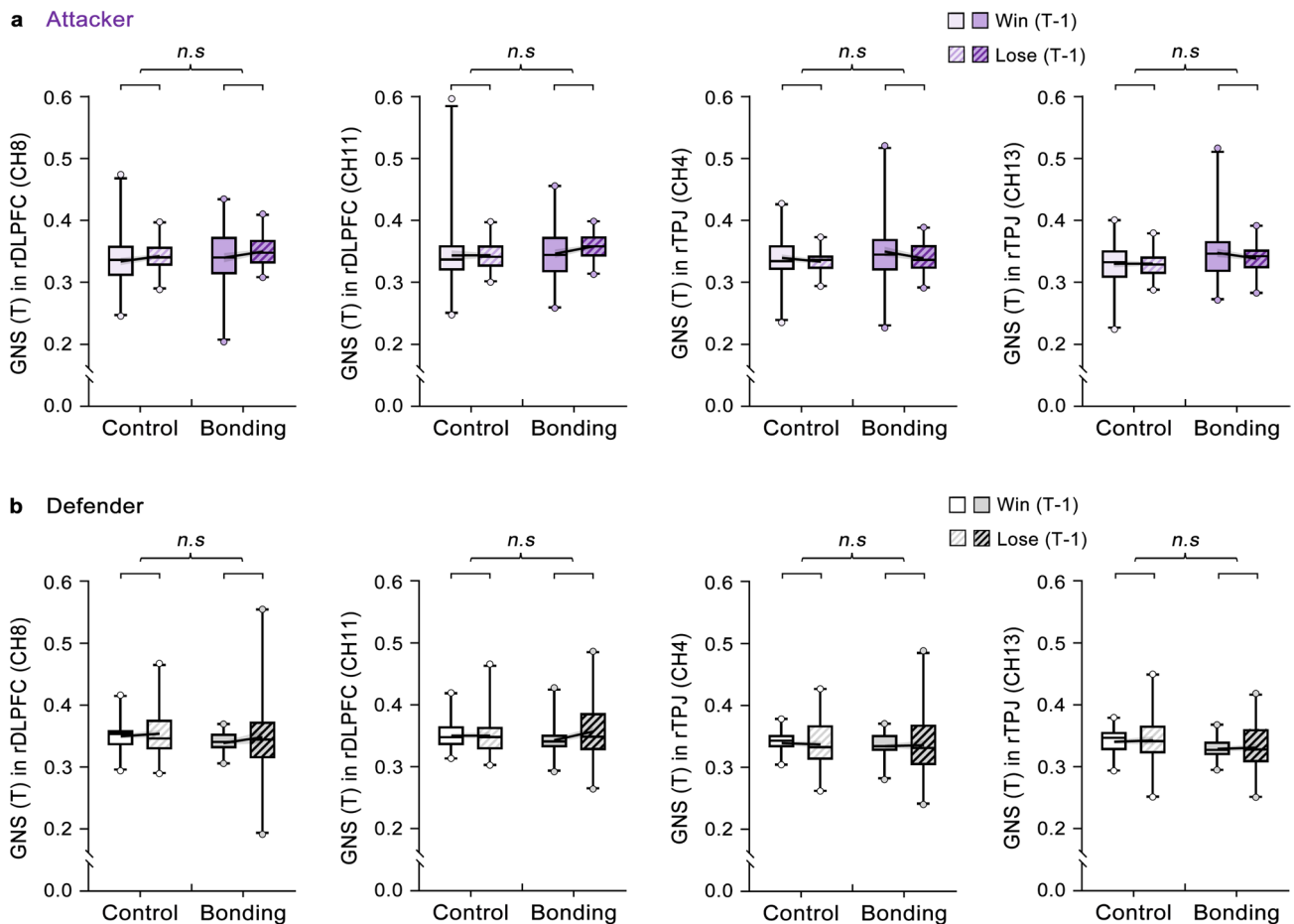
Extended Data Fig. 7 | Within-group Neural Synchronization after Winning or Losing. We compared the GNS after the group won or lost the last round. We conducted Bonding (in-group bonding vs. no-bonding control) × Outcome of last-round T-1 ($win_{(T-1)}$ vs. $lose_{(T-1)}$) mixed-model ANOVAs on GNS of round T. For both attacker (**a**) and defender (**b**) groups, the main effect of Outcome was not significant (**a**, Attacker: channel 8: $F_{1,82} = 3.357$, $p = 0.071$, $\eta^2 = 0.039$; channel 11: $F_{1,82} = 1.164$, $p = 0.284$, $\eta^2 = 0.014$; channel 4: $F_{1,82} = 2.893$, $p = 0.093$, $\eta^2 = 0.034$; channel 13: $F_{1,82} = 0.824$, $p = 0.367$, $\eta^2 = 0.010$; **b**, Defender: channel 8: $F_{1,82} = 1.321$, $p = 0.254$, $\eta^2 = 0.016$; channel 11: $F_{1,82} = 2.100$, $p = 0.151$, $\eta^2 = 0.025$; channel 4: $F_{1,82} = 0.008$, $p = 0.930$, $\eta^2 = 9.39 \times 10^{-5}$; channel 13: $F_{1,82} = 0.183$, $p = 0.670$, $\eta^2 = 0.002$). The Outcome effect was not modulated by in-group bonding (**a**, Attacker: channel 8: $F_{1,82} = 0.019$, $p = 0.890$, $\eta^2 = 2.35 \times 10^{-4}$; channel 11: $F_{1,82} = 1.122$, $p = 0.293$, $\eta^2 = 0.014$; channel 4: $F_{1,82} = 0.244$, $p = 0.622$, $\eta^2 = 0.003$; channel 13: $F_{1,82} = 0.888$, $p = 0.349$, $\eta^2 = 0.011$; **b**, Defender: channel 8: $F_{1,82} = 0.189$, $p = 0.665$, $\eta^2 = 0.002$; channel 11: $F_{1,82} = 1.988$, $p = 0.162$, $\eta^2 = 0.024$; channel 4: $F_{1,82} = 0.124$, $p = 0.725$, $\eta^2 = 0.002$; channel 13: $F_{1,82} = 3.39 \times 10^{-4}$, $p = 0.985$, $\eta^2 = 4.14 \times 10^{-6}$). Data from two sessions were excluded as attackers in these two sessions did not win any of the 24 rounds. Outcome-by-Bonding mixed-model ANOVAs ($n = 84$, 42 three-person groups under no-bonding control and 42 three-person groups under in-group bonding) separately for attacker groups and defender groups. Data are plotted as boxplots for each condition in which horizontal lines indicate median values, boxes indicate 25/75% quartiles, and whiskers indicate the 2.5-97.5% percentile range. Data points outside the range are shown separately as circles. Solid lines start from the mean and reflect the intervals for the Mean ± S.E. *n.s.* not significant.
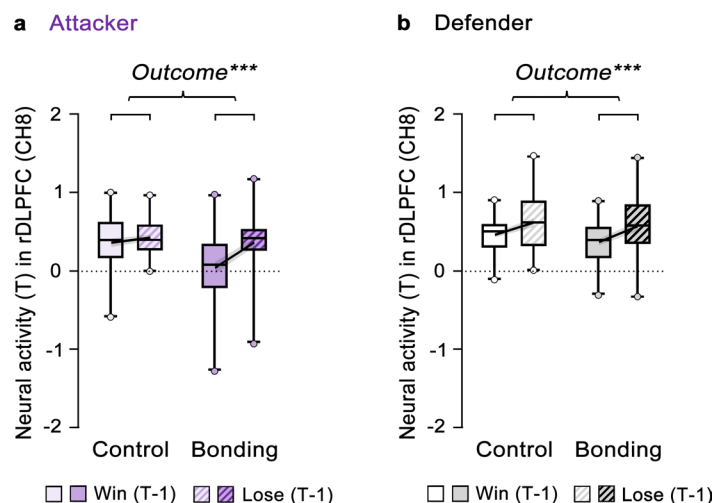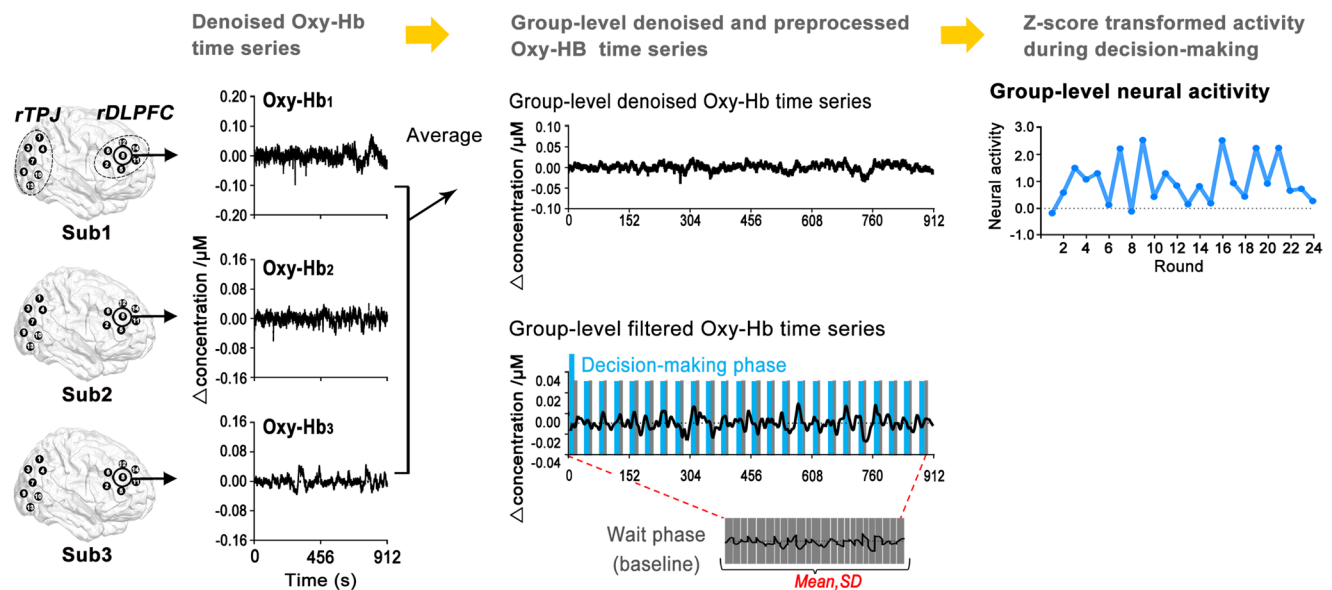
Extended Data Fig. 8 | Within-group Averaged Neural Activity at Channel 8 in the rDLPFC after Winning or Losing. We compared the within-group averaged neural activity in rDLPFC after the group won or lost the last round. We conducted Bonding (in-group bonding vs. control) × Outcome of last-round $T-1$ (win$_{(T-1)}$ vs. lose$_{(T-1)}$) mixed-model ANOVAs on the within-group averaged neural activity of round T. First, we found a significant main effect of Outcome, i.e., stronger neural activity in the rDLPFC during the next-round decision-making phase after the group lost (relative to won) the game, for both the attacker (**a**, channel 8: $F_{1,82} = 29.791$, $p = 5.00 \times 10^{-7}$, $\eta^2 = 0.266$) and defender (**b**, channel 8: $F_{1,82} = 26.595$, $p = 1.71 \times 10^{-6}$, $\eta^2 = 0.245$). Moreover, for the attacker group, we found a significant interaction of Bonding and Outcome on within-group averaged rDLPFC activity (channel 8: $F_{1,82} = 13.207$, $p = 4.85 \times 10^{-4}$, $\eta^2 = 0.139$). Outcome-by-Bonding mixed-model ANOVAs ($n = 84$, 42 three-person groups under no-bonding control and 42 three-person groups under in-group bonding separately for attacker groups and defender groups). Data from two sessions were excluded as attackers in these two sessions did not win any of the 24 rounds. Data are plotted as boxplots for each condition in which horizontal lines indicate median values, boxes indicate 25/75% quartiles, and whiskers indicate the 2.5-97.5% percentile range. Data points outside the range are shown separately as circles. Solid lines start from the mean and reflect the intervals for the Mean ± S.E. ***$p < 0.001$.
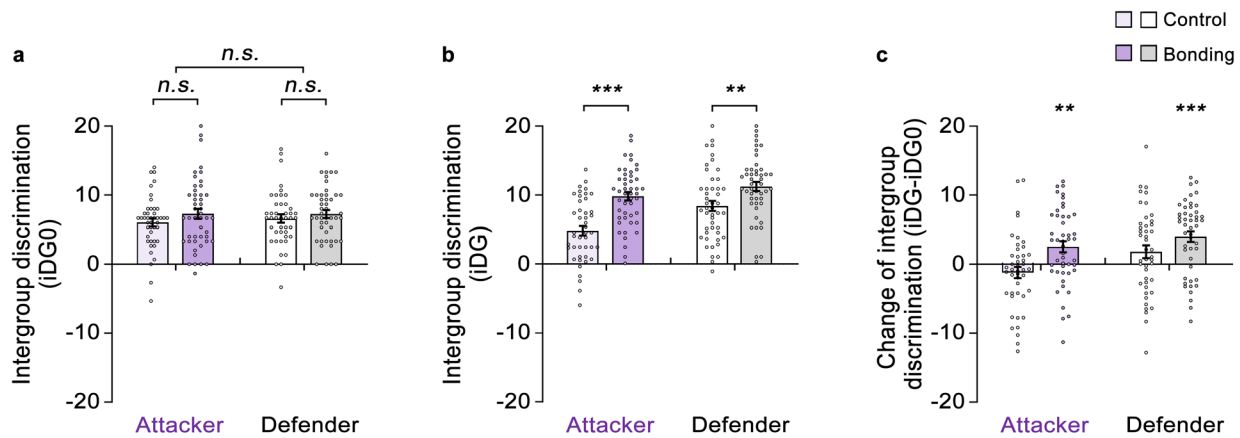
Extended Data Fig. 9 | Effect of In-group Bonding Manipulation on Intergroup Discrimination. We compared in-group bonding index indicated by greater intergroup discrimination (a measure independent of the intergroup contest) before and after the bonding manipulation to quantify the effect of bonding on increasing intergroup discrimination. **a**, Before the bonding manipulation, participants in different conditions showed the same level of intergroup discrimination in the intergroup Dictator Game (iDG) (Bonding: $F_{1,89} = 2.249$, $p = 0.137$, $\eta^2 = 0.025$; Role: $F_{1,89} = 0.181$, $p = 0.672$, $\eta^2 = 0.002$; Bonding × Role: $F_{1,89} = 0.243$, $p = 0.623$, $\eta^2 = 0.003$). Mixed-model ANOVA, $n = 91$ three-versus-three-person intergroup competitions. **b**, In-group bonding (relative to no-bonding control) increased intergroup discrimination in both attacker ($t_{89} = 5.453$, $p = 4.39 \times 10^{-7}$, Cohen's $d = 1.142$, 95% CI = 3.173, 6.812) and defender groups ($t_{89} = 2.788$, $p = 0.006$, Cohen's $d = 0.584$, 95% CI = 0.810, 4.833). Two-tailed independent-samples t-test, 47 three-person attacker (defender) groups under in-group bonding and 44 three-person attacker (defender) groups under no-bonding control. **c**, We directly examined the in-group bonding induced intergroup discrimination by calculating the change from before to after bonding manipulation (i.e. iDG-iDG0). We showed that, in-group bonding manipulation indeed induced a reliable increase in intergroup discrimination ($t_{46} = 7.220$, $p = 4.27 \times 10^{-9}$, Cohen's $d = 1.053$, 95% CI = 2.354, 4.173, two-sided one-sample t-test, 47 three-versus-three-person intergroup competitions under in-group bonding condition), which was observed in both attacker ($t_{46} = 3.171$, $p = 0.003$, Cohen's $d = 0.463$, 95% CI = 0.925, 4.140, two-sided one-sample t-test, 47 three-person attacker groups) and defender groups ($t_{46} = 5.222$, $p = 4.16 \times 10^{-6}$, Cohen's $d = 0.762$, 95% CI = 2.455, 5.534, two-sided one-sample t-test, 47 three-person defender groups). In addition, under no-bonding control condition, there was no change of intergroup discrimination for attacker ($t_{43} = -1.464$, $p = 0.150$, Cohen's $d = -0.221$, 95% CI = −2.867, 0.455, two-sided one-sample t-test, 44 three-person attacker groups) or defender groups ($t_{43} = 1.936$, $p = 0.059$, Cohen's $d = 0.292$, 95% CI = −0.075, 3.692, two-sided one-sample t-test, 44 three-person defender groups). Data showed as Mean ± S.E. with overlaid dot plots. **$p < 0.01$, ***$p < 0.001$, n.s. not significant.
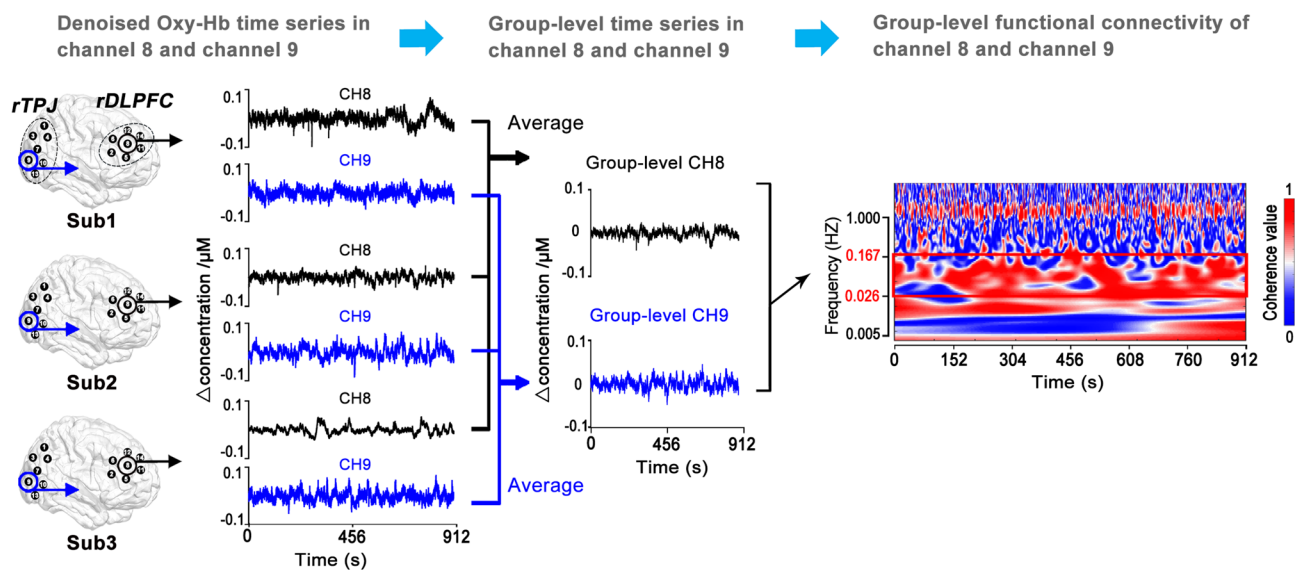
Extended Data Fig. 10 | Illustration of group-level neural activity and rDLPFC-rTPJ connectivity calculation. a, Different from group-averaged neural activity in Extended Data Fig. 5, we calculated the group-level neural activity by first averaging the denoised Oxy-Hb neural activity across 3 participants of each pseudo groups. The group-level, preprocessed Oxy-Hb time series of each channel were then segmented into 3 conditions, i.e., the decision-making phase, the waiting screen, and the outcome screen. The pre-processed, group-level Oxy-Hb during decision-making (outcome) phase was z-score transformed using the mean value and standard deviation of the group-level waiting period (as baseline) and indicated group-level decision-making (outcome) related activity. **b,** The group-level function connectivity between rDLPFC and rTPJ was calculated by first averaging the denoised Oxy-Hb neural activity in each channel across 3 participants of each group. We then performed coherence analyses between each of the 7 channels in the rDLPFC with each of the 7 channels in the rTPJ (i.e., 49 channel pairs) to index channel-pairwise group-level functional connectivity (GFC) of rDLPFC–rTPJ. We also calculated at the grand mean level (i.e., the averaged coherence value of 49 channel pairs) to index grand mean group-level functional connectivity.

Corresponding author(s): Yina MA

Last updated by author(s): Mar 18, 2020

Reporting Summary

Nature Research wishes to improve the reproducibility of the work that we publish. This form provides structure for consistency and transparency in reporting. For further information on Nature Research policies, see Authors & Referees and the Editorial Policy Checklist.

Statistics

For all statistical analyses, confirm that the following items are present in the figure legend, table legend, main text, or Methods section.

n/a	Confirmed	
☐	☒	The exact sample size (*n*) for each experimental group/condition, given as a discrete number and unit of measurement
☐	☒	A statement on whether measurements were taken from distinct samples or whether the same sample was measured repeatedly
☐	☒	The statistical test(s) used AND whether they are one- or two-sided *Only common tests should be described solely by name; describe more complex techniques in the Methods section.*
☐	☒	A description of all covariates tested
☐	☒	A description of any assumptions or corrections, such as tests of normality and adjustment for multiple comparisons
☐	☒	A full description of the statistical parameters including central tendency (e.g. means) or other basic estimates (e.g. regression coefficient) AND variation (e.g. standard deviation) or associated estimates of uncertainty (e.g. confidence intervals)
☐	☒	For null hypothesis testing, the test statistic (e.g. *F*, *t*, *r*) with confidence intervals, effect sizes, degrees of freedom and *P* value noted *Give P values as exact values whenever suitable.*
☒	☐	For Bayesian analysis, information on the choice of priors and Markov chain Monte Carlo settings
☒	☐	For hierarchical and complex designs, identification of the appropriate level for tests and full reporting of outcomes
☐	☒	Estimates of effect sizes (e.g. Cohen's *d*, Pearson's *r*), indicating how they were calculated

Our web collection on statistics for biologists contains articles on many of the points above.

Software and code

Policy information about availability of computer code

Data collection	LABNIRS-1 20set , MATLAB R2014b and custom matlab code
Data analysis	MATLAB R2019a and custom matlab code

For manuscripts utilizing custom algorithms or software that are central to the research but not yet described in published literature, software must be made available to editors/reviewers. We strongly encourage code deposition in a community repository (e.g. GitHub). See the Nature Research guidelines for submitting code & software for further information.

Data

Policy information about availability of data

All manuscripts must include a data availability statement. This statement should provide the following information, where applicable:

- Accession codes, unique identifiers, or web links for publicly available datasets
- A list of figures that have associated raw data
- A description of any restrictions on data availability

All behavioral data and materials have been made publicly available via the Open Science Framework and can be accessed at: https://osf.io/uh3sx/. The neural data and code that support the findings of this study are available from the corresponding author upon reasonable request.

Field-specific reporting

Please select the one below that is the best fit for your research. If you are not sure, read the appropriate sections before making your selection.

☒ Life sciences   ☐ Behavioural & social sciences   ☐ Ecological, evolutionary & environmental sciences

Life sciences study design

All studies must disclose on these points even when the disclosure is negative.

Sample size	The sample size was determined a priori using G*Power 3.1 (Ref 51) to estimate the number of six-person sessions needed to detect significant effects with 80% statistical power. We originally considered conducting power analysis based on both behavioral and neural effects. However, most fNIRS studies have considered dyad-level interactions, and only a few have examined neural synchronization in single groups with group sizes n ≥ 3, and we are unaware of fNIRS studies examining intergroup (economic) interaction. We thus calculated a priori sample size estimates on the basis of earlier behavioral studies using the intergroup contest that we also used here. Based on a small-to-medium effect size estimated by a meta-analysis on the effect of in-group bonding on intergroup discrimination in cooperation (Cohen's d = 0.32), 80 six-person sessions were needed to detect a reliable effect with α = 0.05, β = 0.80 for a within (attacker vs. defender) by between (in-group bonding vs. control) treatment interaction. To allow for drop-out due to technical failure, we recruited 93 sessions.
Data exclusions	Similar to previous studies (Ref 18) excluding groups based on data collection failure, in our study, two six-person contest sessions were excluded because of a technical failure to record contribution decisions, leaving 546 participants in 91 contest sessions(40 male sessions, Mean ± SD = 22.04 ± 1.31 years; Supplementary Table 1a) for behavioral data analysis. Another 5 six-person contest sessions were excluded because of technical failure with fNIRS measurements, leaving a total of 516 participants in 86 intergroup contest sessions for neural data analysis (38 male sessions, Mean ± SD = 22.01 ± 1.29 years; Supplementary Table 1b).
Replication	The experiment was performed once, and no replication experiments were conducted. The manuscript contains all information necessary to conduct replication experiment. The main analyses were performed on the populational level, in which case the variation in subject responses was incorporated into statistical testing. The variability in behavioral and neural responses is shown through the plotting of individual data or data range in all the figures. The result of the Deoxy-Hb signals was found similar as those reported for oxygenated hemoglobin (Oxy-Hb) signals. All of the main findings remain the same before and after applying wavelet-based global noise removal, and when controlling for the global mean as a covariate. The main effect of group role on behavioral measures (higher contribution and higher decision coordination for defender than attacker) replicated previous finding
Randomization	All participants were randomly assigned to the in-group bonding or no-bonding control manipulation, and randomly assigned to the group role of attacker or defender.
Blinding	The Role (attacker vs. Defender) was randomly assigned and blind to the experimenter during data collection. Data analysis was not performed blind to the conditions of the experiments.

Reporting for specific materials, systems and methods

We require information from authors about some types of materials, experimental systems and methods used in many studies. Here, indicate whether each material, system or method listed is relevant to your study. If you are not sure if a list item applies to your research, read the appropriate section before selecting a response.

Materials & experimental systems

n/a	Involved in the study
☒	☐ Antibodies
☒	☐ Eukaryotic cell lines
☒	☐ Palaeontology
☒	☐ Animals and other organisms
☐	☒ Human research participants
☒	☐ Clinical data

Methods

n/a	Involved in the study
☒	☐ ChIP-seq
☒	☐ Flow cytometry
☒	☐ MRI-based neuroimaging

Human research participants

Policy information about studies involving human research participants

Population characteristics	Healthy individuals (N = 558, 252 males, age 18-30 years, Mean ± SD = 22.06 ± 2.58 years) were invited as paid volunteers. All participants had normal or corrected-to-normal vision and no history of neurological or psychiatric disorders. Behavioral data analyses were conducted on 91 three-versus-three-person intergroup competition sessions (40 males sessions, Supplementary Table 1a). Neural data analysis was conducted on 86 three-versus-three-person intergroup sessions (Supplementary Table 1b). The attacker and defender groups under in-group bonding or no-bonding control conditions did not differ in gender, age, education, empathic capacity, cooperative personality, social-value orientation, prosocial personality,impulsiveness, justice sensitivity, preference for social hierarchy, and baseline intergroup discrimination (detailed Supplementary Table 1)
Recruitment	558 healthy individuals were recruited in this study as paid volunteers through on campus flyer recruitment. No self-selection biases was involved in the participant recruitment.

Ethics oversight | The experimental protocols adhered to the standards set by the Declaration of Helsinki and was approved by a local Research Ethics Committee at the State Key Laboratory of Cognitive Neuroscience and Learning, Beijing Normal University Beijing, China (protocol number: IORG0004944).

Note that full information on the approval of the study protocol must also be provided in the manuscript.